Final Report: Individual Electro-Hydraulic Drives for Off-Road Vehicles

award # DE-EE0008334

PI: Andrea Vacca (Purdue University)
Co-PIs: Dr. Scott Sudhoff (Purdue University)
Uwe Neumann (Bosch Rexroth),
Gary Kassen (Case New Holland Industrial)

August 30th, 2022

U.S. DEPARTMENT OF ENERGY

PURDUE UNIVERSITY

Contents

1 Introduction 2

2 Budget period 1 7

2.1 Reference vehicle definition 7

2.2 EH module design & simulation model 9

2.3 Electro-hydraulic unit designs 15

2.4 1st generation simulation models and optimization procedure 15

2.4.1 Objective function 18

2.4.2 Constraints 20

2.4.3 Results 21

2.4.4 Axial compensation system design 22

2.5 2nd generation morphology definition 23

3 Budget period 2 25

3.1 EH module test & verification 25

3.2 EH manufacturing and experimental test 29

3.3 EH module demo with EH unit 33

4 Budget period 3 35

4.1 EH module implementation 35

4.2 Vehicle demonstration and performance 37

4.3 IGM model 43

4.4 2nd generation EHU design 44

4.4.1 IGM Power Loss Calculator 45

4.4.2 IGM gears profile optimization 45

4.4.3 IGM morphology and cooling system 47

4.4.4 IGM manufacturing and testing 49

4.5 EHU design conclusion 52

1 Introduction

This document constitutes the final report of the project titled "Individual Electro-Hydraulic Drives for Off-Road Vehicles" (DOE award # DE-EE0008334). The project started May 1st 2018 and ended May 31st 2022. There were three budget periods (BPs) that, considering no-cost extension made throughout the project, had following periods:

BP1 – Preliminary design: 05/01/2018 – 07/31/2019

BP2 – Initial implementation: 08/01/2019 – 01/31/2021

BP3 – Technology demonstration: 02/01/2021 – 05/31/2022

A good overview of the scopes and milestones of each BP is given by the Tab. 1 at the next page. The table outlines the target and go/no go decision points of each BP, which were used to assess the project results and determine the continuation through subsequent BPs.

The main objective of the project was to develop and demonstrate an electro-hydraulic technology that, with respect to current state of the art solutions for off-road vehicles, can:

1. Lower power consumption of the fluid power system up to 70%
2. Reduce noise emissions and vibration
3. Allow for zero emission operation of the vehicle (engine off operation)
4. Enable "smart actuators" operating as modern "plug & play" elements with integrated control and self-diagnostic functions.

The above target 1. is the key of the proposed activities, as the project mainly addresses the low consumption of current state of the art technology for off-road vehicles. Most of the activities and of the designed project milestones are around meeting the energy efficiency target. The other advantages 2., 3., 4. of the proposed technology are inherent to the proposed electrification solution, and the scalability of the design, as it will be further illustrated in this report.

The basic representation of the proposed system can be found in Figure 1. Essentially, the project proposes a modular "flow on demand" schematic used to control any hydraulic function of the machine, starting from an electric supply (i.e. battery system). Therefore, the solution is meant to enable efficient battery powered off-road vehicles.

The project activities to develop such systems embraced both simulation and experimentation, and they were divided into three areas:

O1. Four-quadrant electro-hydraulic unit (EHU) design

O2. Individualized electro-hydraulic system

O3. Technology demonstration

Period 1 (12 months) Preliminary Design	Period 2 (12 months) Initial Implementation	Period 3 (12 months) Technology Demonstration
Description		
numerical analysis for the EH units (O1), as well as for the individualized system (O2). Identification of the best design solutions and the related performance parameters (energy efficiency, power-to-weight ratios, costs). Determination of the requirements of the electric system of the overall vehicle considering the typical duty cycles for both reference vehicle.	initial prototypes of EH units will be tested for model validation and refinement. Individual EH unit prototypes will be fabricated and tested using standard components for the electric motor and the 4-quadrant hydraulic unit. Functionality tests will be performed.	Prototypes of the EH units will be fabricated and as tested stand-alone and for the boom and bucket functions of a wheel loader – demo vehicle 2. Plug & play communication as well as self-diagnostic features will be demonstrated on the individual EH unit, and optimal energy-management strategies will be studied for the entire electric-hydraulic hybrid system.
Milestones		
A. Definition of demo vehicles (O3) B. EH-unit, EGM (O1) C. EH-unit, internal gear (O1) D. EH module layout (O2)	E. 4-quadrant EH unit design (O1) F. 4-quadrant EH unit test (O1,O2) G. Demo vehicle tests (O3)	H. EH unit general design rules (O1) I. EH unit design (2nd gen) (O1) J. EH module final design (O2) K. Demo vehicle results (O3)
Go/No Go decision points (to proceed with the planned activities of the next project period)		End of project goals
GNG1. EH module simulated performance above 0.75 at best point. EH unit efficiency (above 0.8 at best points)	GNG2. Experimentally validate functionality of 4-quadrant EH unit with measured efficiency greater than 0.5. Demo performance (the measured energy efficiency of the hydraulic system) at least 20% higher than the commercial solution	END1. Design formulation for integrated EH units (O1) END2. Prototypes for independent EH modules with integrated control and diagnostic function (O2) END3. Functional off-road demo vehicle available at Purdue END4. Improved fuel economy demonstrated from demo vehicle test

Table 1: Main specifications of the reference vehicle

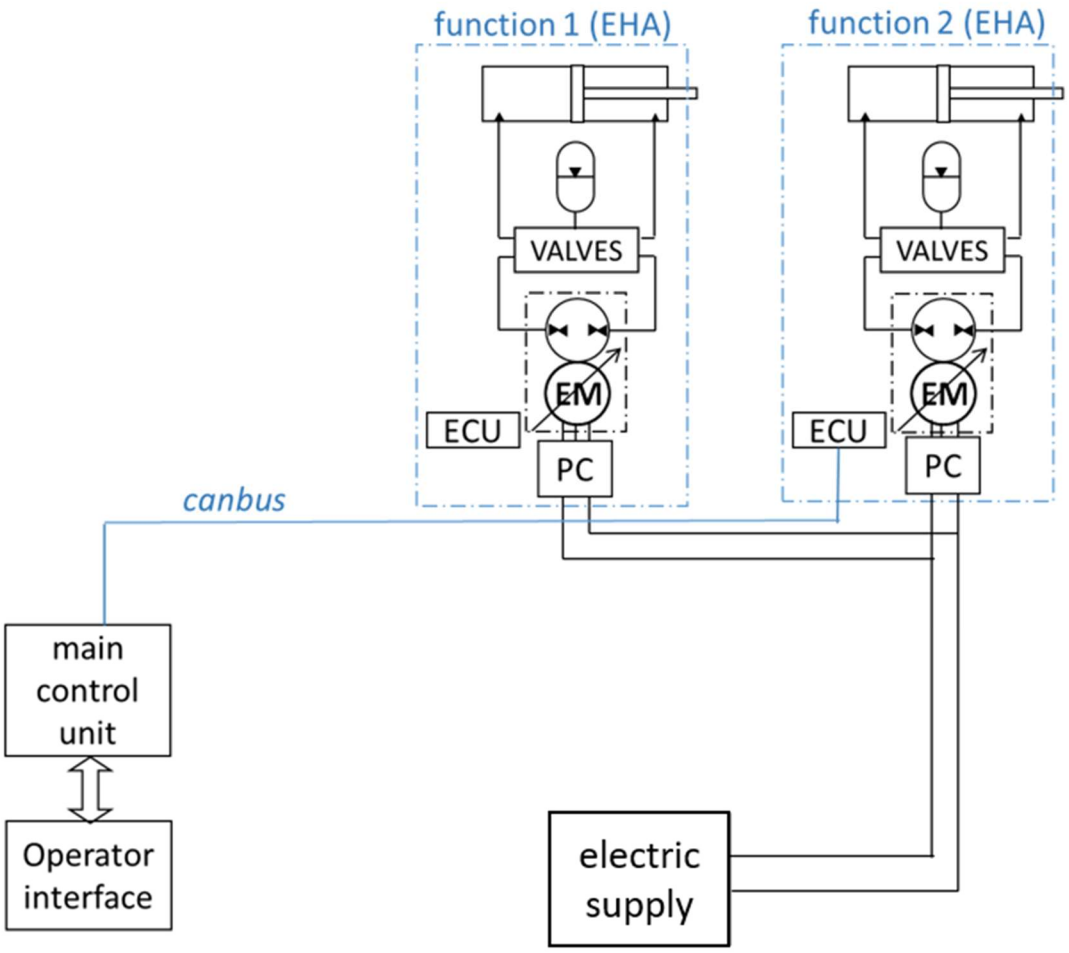

Figure 1: Schematic idea of the proposed system

Within O1, the project developed the key element of the actuation system, which is the electro-hydraulic pump/motor (EHU). The project particularly aimed at developing a solution that integrates the electric machine and the hydraulic machine in a single housing, in such a way that energy efficiency, weight, volume and magnetic material could be optimized. Such units can also operate to recover energy from overrunning loads. Two different architectures for the hydraulic machines were taken into consideration (i.e. external gear unit and internal gear unit), to be combined with efficient permanent magnet electric machines.

Within O2, the project formulated and demonstrated the layout of the hydraulic control system that maximizes the benefits of the EHU. Several architectures for such system were considered, such as open circuit and closed circuit, and assessed with respect to energy efficiency, functionality and ease of implementation.

Milestone BP1	Type	Description
Demonstration Vehicles Defined	Technical	The physical vehicles used for demonstrations will be identified and set up.
EGM EH-Unit Design Architecture Completed	Technical	The design architecture of the EH unit, inclusive of hydraulic unit and electric motor, is finalized for the case of EGM.
4-Quadrant Hydraulic Unit Architecture Completed	Technical	The design architecture of the EH unit, inclusive of hydraulic unit and electric motor, is finalized for the case of internal gear machine.
EH-Module Layout Finalized	Technical	The hydraulic layout architecture for the EH module is finalized.
EH Simulated Performance Measured	Go/ No Go	Simulated performance of the EH module (with/without accumulator) is completed. The overall efficiency of the EH module is confirmed to be above 0.75 at best points. The EH unit simulated efficiency is confirmed to be greater than 0.6 (0.8 at best efficiency points).

Milestone BP2	Type	Description
4-Quadrant EH Unit Design Complete	Technical	Fully integrated 4-quadrant unit design is completed
4-Quadrant EH Unit Test	Technical	Prototypes of the hydraulic units as well as the electric motors are fabricated and tested
Demo vehicle tests	Technical,	The EH module prototype is installed and tested on a relevant application
Quadrant EH Unit Demo and Vehicle Performance	Go/No Go	EH Unit tests validate functionality with a minimum efficiency greater than 0.5. Measured energy efficiency of the hydraulic system on demo vehicle 1 needs to be at least 20% higher than the commercial system

Milestone BP3	Type	Description
EH-unit general design rules	Technical	Rules and guidelines for designing integrated 4-quadrant units will be ready to be disclosed.
EH-unit design (2nd gen)	Technical	The 2nd generation design study of the 4-quadrant EH unit is completed.
EH module final design	Technical	The design of fully integrated EH modules with self-diagnostic function is completed.
Demo Vehicle results	Technical	Productivity tests on the wheel loader are completed. Efficiency and fuel consumption is compared to the commercial vehicle.

Table 2: Milestones and Go/No Go points for the different budget periods

Within O3, the project experimentally demonstrated the technology on a dedicated test rig and on a reference vehicle. The case of a compact skid steer loader was considered as representative of a large market of the off-road vehicles produced and sold in the U.S.

The project milestones were listed in Tab. 1 but are further detailed in Tab. 2.

The project team consisted of:

- Purdue University (lead).
  The research teams of Dr. Vacca (PI) and Dr. Sudhoff were part of the effort. Dr. Vacca supervised the entire project activities, and his team was in charge of the experimental and simulation activities concerning the hydraulic system. These activities were performed at the Maha Fluid Power Research Center of Purdue University, which is the largest academic research center dedicated to research in fluid power in the U.S. Dr. Sudhoff's team was in charge of the activities related to the electric machine design and control. An average of 3.5 graduate students were constantly involved in this effort during the duration of the project.

- Bosch Rexroth.
  Lead initially by Dr. Newman, and later by Dr. Busquets, the Bosch Rexroth team assisted the activities related to the fabrication of the hydraulic machine components, the EHU integration providing also the components and the technical data necessary to drive the experimental and the validation activities. Bosch Rexroth also assisted in the cost analysis for making considerations suitable for the future commercialization of the EHU as well as of the entire actuation system.

- Case New Holland Industrial (CNH).
  CNH provided the reference vehicle and related drive cycle data necessary to properly perform the sizing activities for the component. Assistance towards the actual implementation of the test set up, in both the stationary test rig and in the on-vehicle implementation was provided by the team led by Kassen.

The Team member met with a bi-monthly frequency or higher to discuss the progress of the project and for planning the details of the project activities.

The total cost of the project was $ 1,919,142 of which $1,500,000 of federal share.

Seventeen (17) quarterly progress reports were submitted by the Team, as required by the project agreement, in addition to the annual progresses and two continuation applications submitted to initiated BP2 and BP3 respectively. Project details were also discussed during the quarterly review meetings involving the DOE Program Manager.

This present document provides a general overview of the project activities. The explanations will be provided following the order of the project milestones of Tab 2, so that the main activities and accomplishments related to each milestone can be clearly delivered. More details on each activity performed can also be found on the quarterly progress reports mentioned above.

2 Budget period 1

In this chapter, the work in budget period 1 (BP1) is summarized based on milestones in the first year accordingly. The following sections include the technical milestones in terms of the EH module and EH unit, and the Go/No Go (GNG) milestone for the system performance is highlighted with results.

2.1 Reference vehicle definition

This paragraph describes the accomplishment of the milestone named "Demonstration Vehicle Defined".

The reference vehicle in this study is defined as a skid steer compact loader from CNH industrial. The machine CASE TV380 is commonly employed in present market, so it can represent the commercial off-road applications. Figure 2 gives a picture of the reference vehicle taken in the Maha Fluid Power Research Center, Purdue University.

Figure 2: Reference vehicle defined for this project

Table 3 shows the main specifications of the reference vehicle about the engine, power level, hydraulic flow requirements, etc.

In this project, two functions of actuating boom and bucket are considered for the technology demonstration. The reference machine was fully instrumented, such as pressure/displacement sensors, for baseline measurements of hydraulic power consumption. Typical machine duty cycles are provided by CNH, based on which the test plan was executed.

Table 3: Main specifications of the reference vehicle

Machine Main Specification	
Engine Type	Diesel, Turbo – Direct Injection,4 cylinders
Max power	90 hp [67 kW]
Fuel Capacity	25.5 gal [96.5 L]
Max Standard flow	24.2 gpm [91.5 L/min]
Machine Weight	10,207 lb [4630 Kg]
Engine speed	1150-2500 rpm

Figure 3 shows the measured data of one duty cycle, including the displacement of the actuator, pump input power, load force applied on the actuator, and the pressure in the cylinder chamber. The reference machine utilizes open-center hydraulic systems to control the boom and bucket. This layout has good controllability but low efficiencies due to throttling losses. One typical condition is when lowering the boom without load, the operator needs to push the boom against the meter-out orifice, resulting in the high throttling losses and lack of energy regeneration. More details and explanation on this scenario can be found in the previous reports.

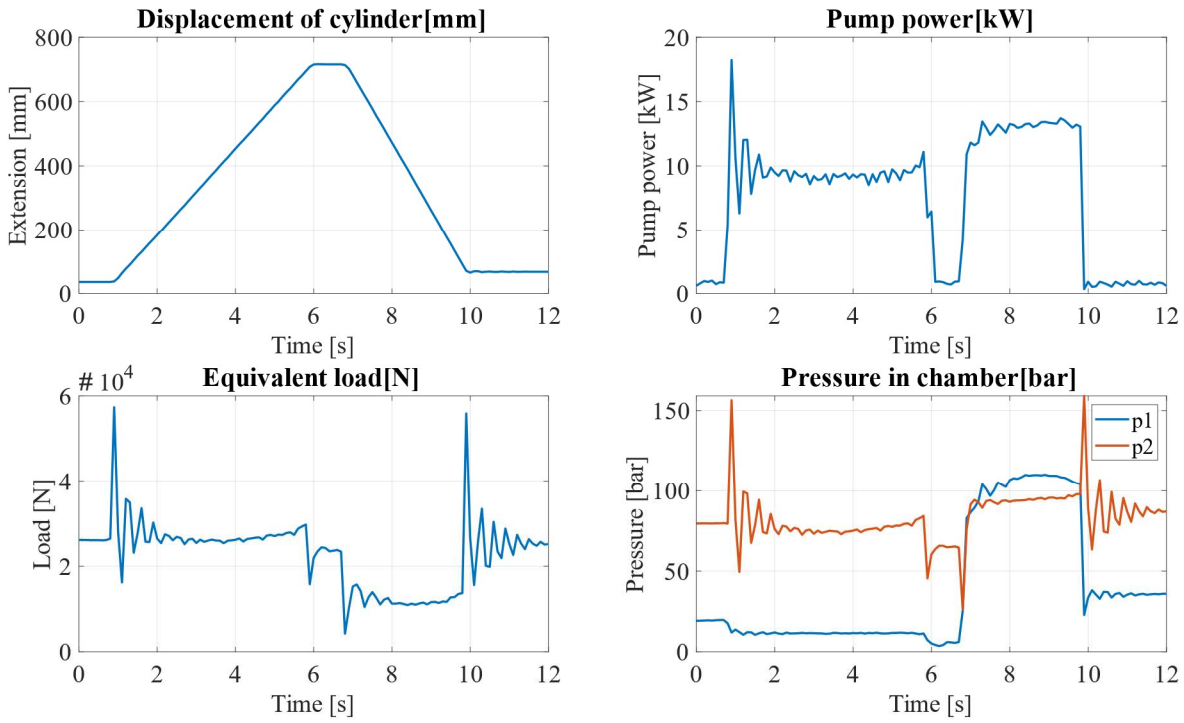

Figure 3: Baseline measurement of one typical duty cycle

2.2 EH module design & simulation model

This paragraph describes the accomplishment of the milestone named "EH-Module Layout Finalized" and "EH Simulated Performance Measured".

Two layouts are proposed as the EH module final design candidates: including an open-circuit design, as shown in Figure 4; and a closed-circuit design represented in Figure 5. Both layouts can achieve 4-quadrant operation of the actuator in terms of loading force and actuation velocity, but with some difference in design topology. The open-circuit layout uses a 2-quadrant hydraulic machine, and the 4-quadrant modes switch reply on the directional valve (4/3 DV). The closed-circuit layout uses a 4-quadrant hydraulic machine instead, so the operation in 4-quadrant can be achieved directly, and the valves are mainly for on/off of the hydraulic system.

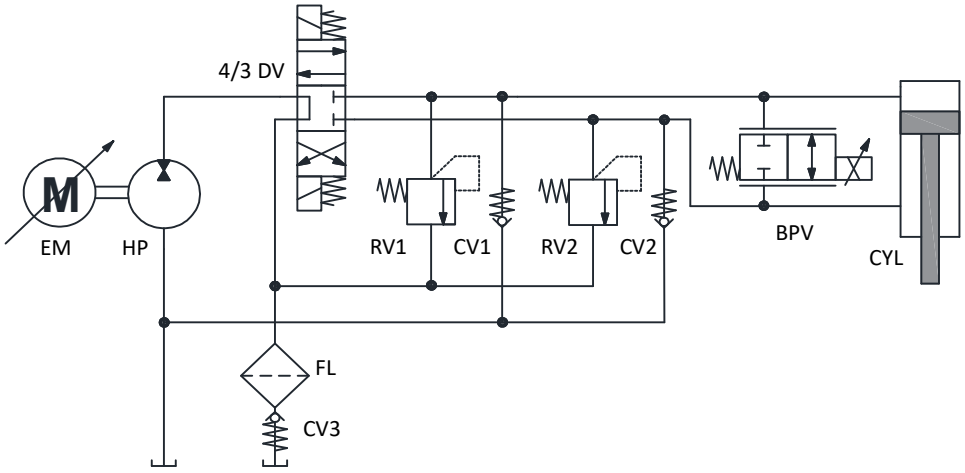

Figure 4: EH module layout: open-circuit design

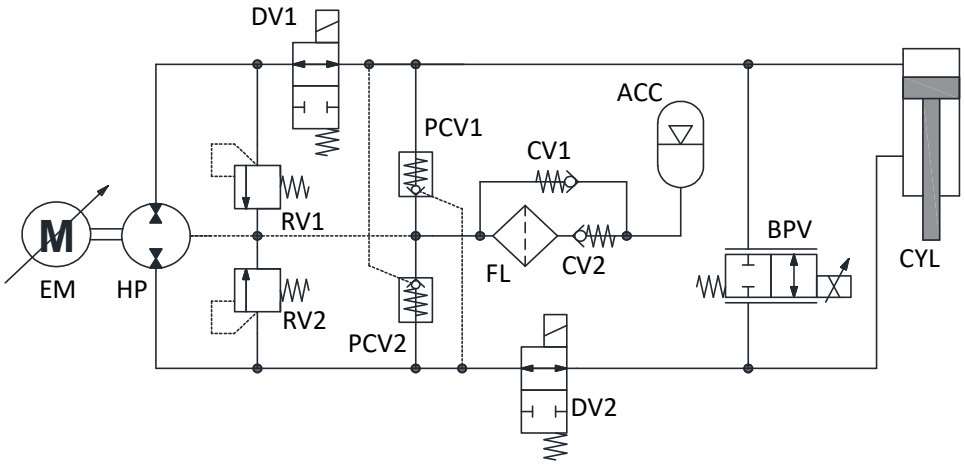

Figure 5: EH module layout: closed-circuit design

One challenge of such design is the low-speed operation control: the actuation velocity depends on the flow rate delivered by the fixed-displacement hydraulic machine, which is not recommended to run under low speed (wear and performance reasons). Therefore, the low-speed range could be a gap in such layouts with the pump speed control strategy. To address this challenge, a novel layout with the bypass valve (BPV) is proposed. The BPV is located parallel to the cylinder in both layouts and can recycle flow to achieve low-speed operation.

Figure 6 shows the operation modes in four-quadrant, taking the closed-circuit as an example. The working principle of the open-circuit layout is similar. In most cases, the BPV keeps closed to minimize throttling losses, and the actuation velocity is fully controlled by the flow rate delivered by the pump, equally the speed of the electric machine. The accumulator helps to compensate the differential flow from the cylinder.

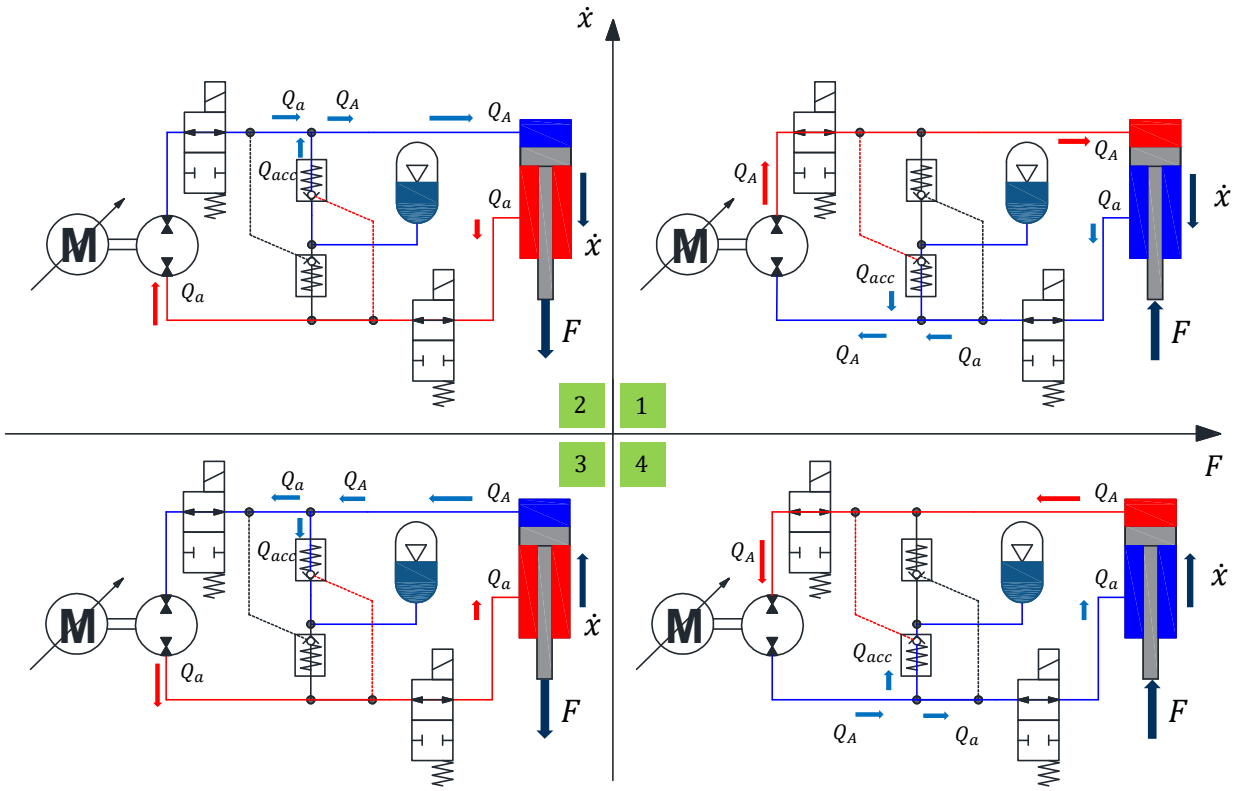

Figure 6: Four-quadrant operation modes of closed-circuit layout

Figure 7 shows the detailed working modes with the bypass valve, with the open-circuit layout 3 and 4 quadrant as an example. In low-speed mode, the fixed-displacement pump is set at the minimum speed in resistive case, or zero speed in assistive case, while the bypass valve recycle flow to the cylinder chamber to achieve speed control. Furthermore, the bypass valve allows a fast retraction mode, with the pump reaching the maximum speed, the BPV can be opened to increase the actuation velocity. This mode is specifically helpful to avoid oversizing the EH module and the EH unit working as the prime mover.

Figure 8 summarizes the four-quadrant modes: normally the system relies on the speed control of the pump with high efficiency. Under low-speed mode the bypass valve is used, and in fast retraction condition the bypass valve can be used again to address the sizing gap of the system.

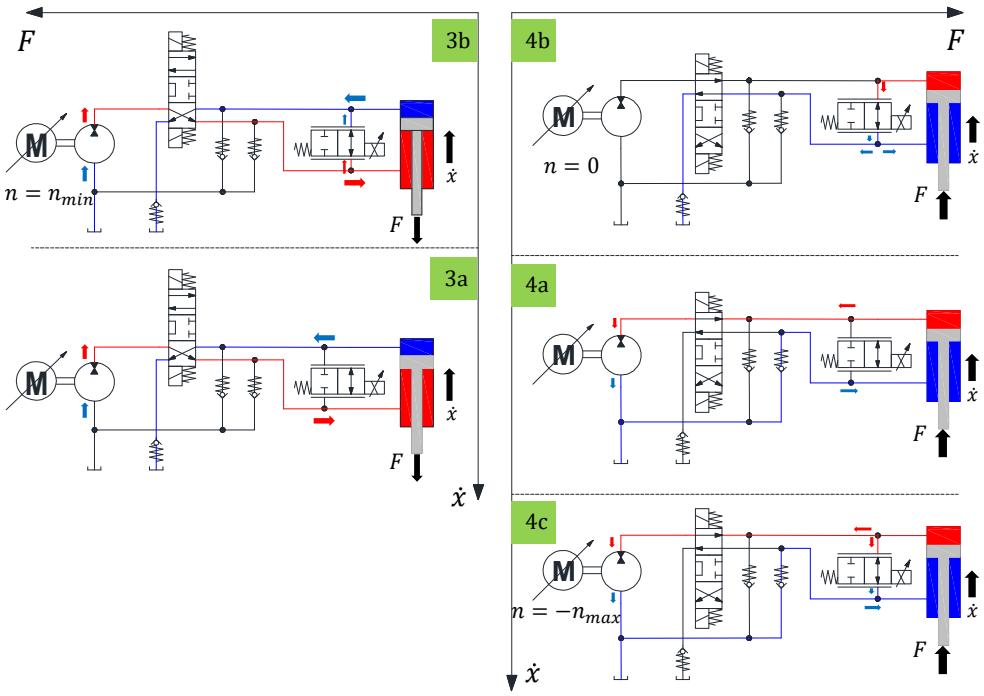

Figure 7: Working principle of bypass valve in 3&4 quadrants

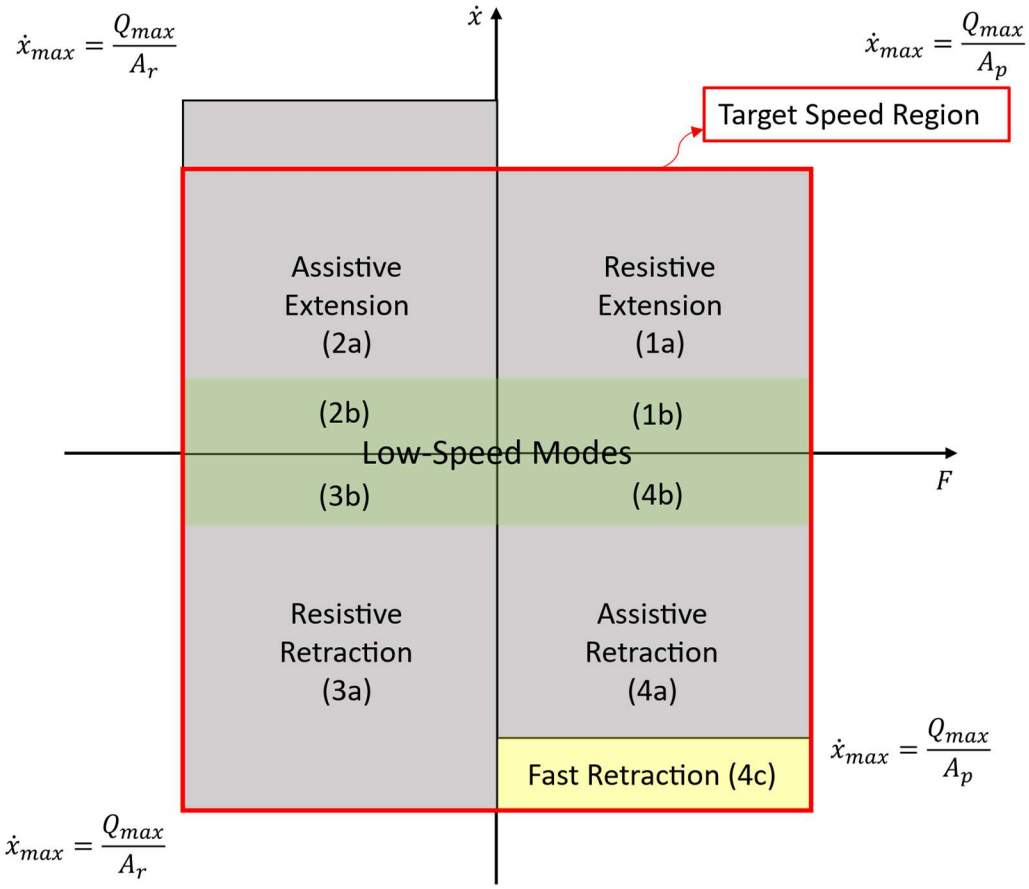

Figure 8: Summary of the four-quadrant modes

Regarding the simulation model, Figure 9 gives a screenshot of the lumped-parameter model developed in Simcenter Amesim, including the electric machine, hydraulic system, and the mechanism such as the boom actuation system. The model includes information about the system performance, including the efficiency map of the electric/hydraulic machine, pressure-flow curve of the hydraulic valves, mass and gravity center of the boom mechanism, etc. With such information, the simulation model can predict the system efficiency performance and detailed power losses in each element of the system. The baseline data with duty cycle information can work as the input to the model.

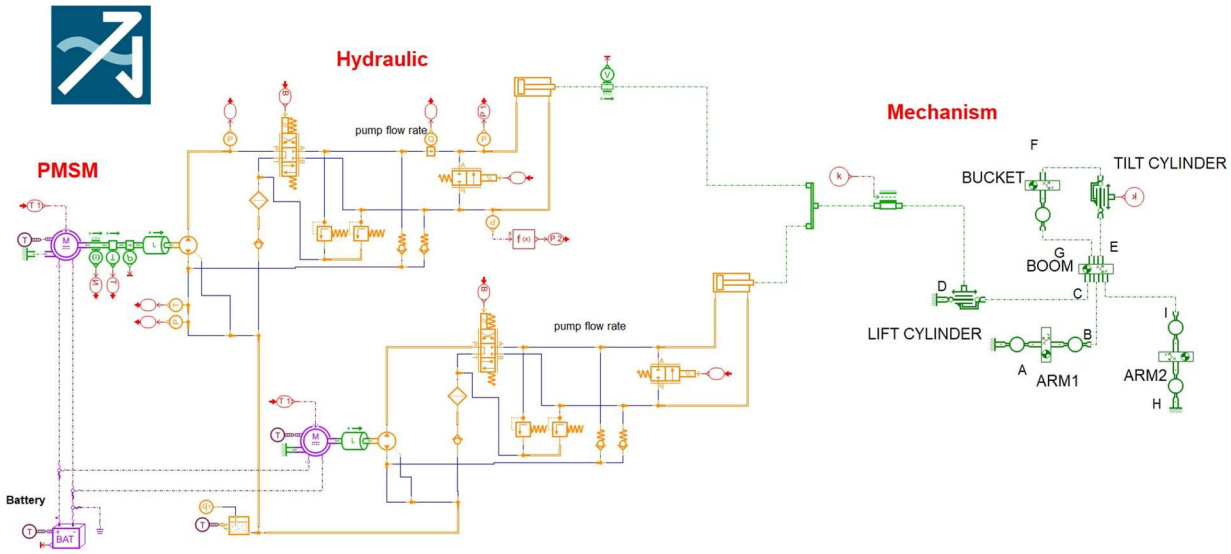

Figure 9: Simulation model developed in AMESIM platform

Figure 10 shows the synchronous motion of the measurements and simulation. The baseline data are input to the model, and the simulation can generate animations to reflection the real cycles.

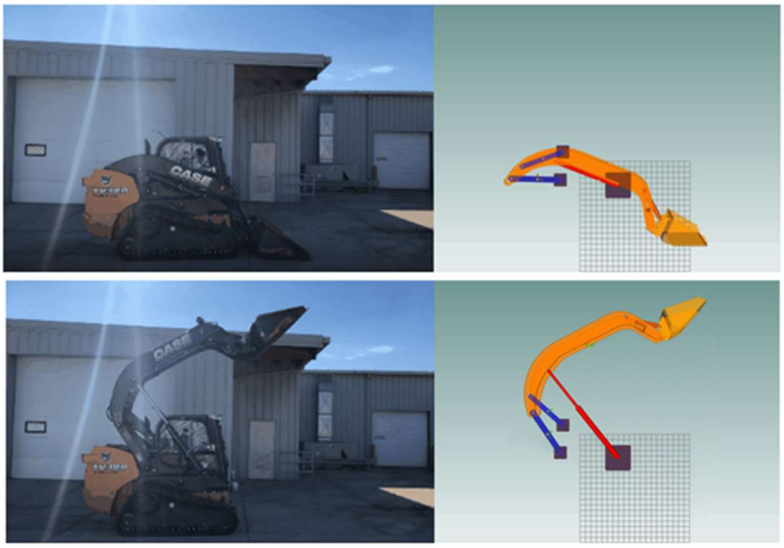

Figure 10: Synchronous motion: baseline measurements vs simulation

In terms of the simulation results, Figure 11 gives the efficiency map in four-quadrant of the overall system, including the inverter, electric machine, hydraulic machine and circuit. The best efficiency is more than 80%, thus achieving the GNG milestone for BP1.

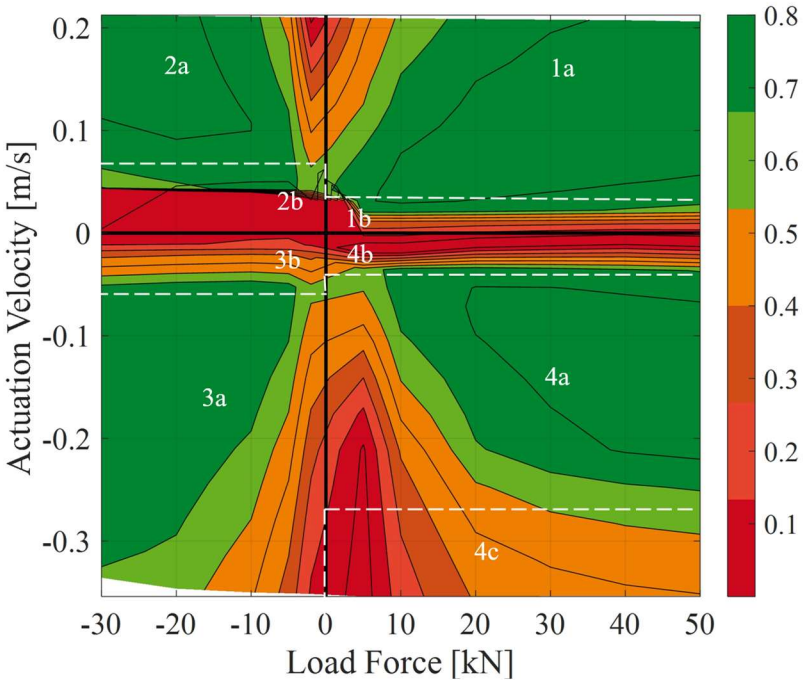

Figure 11: Simulated efficiency map of the overall system

Figure 12 gives the results of energy saving in one duty cycle from the simulation. The saving is up to 80% and achieve the GNG milestone as well. The open-circuit layout performs better due to the better efficiency performance of the 2-quadrant pump compared to the 4-quadrant one in the closed-circuit architecture.

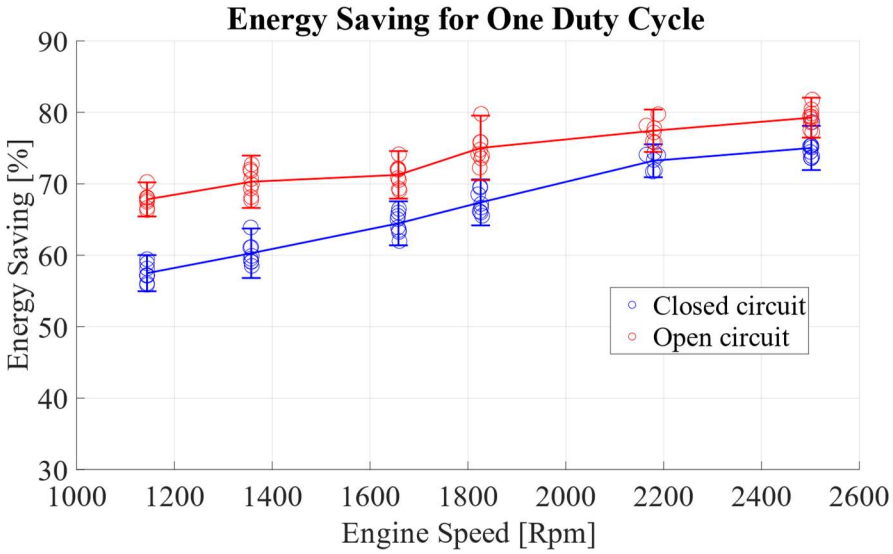

Figure 12: Simulated energy saving in one duty cycle compared to baseline

2.3 Electro-hydraulic unit designs

A crucial task of the project is the design of the electro-hydraulic drive for the actuator. The PI designed 2 different versions of EHU, which will be referred as 1st generation and 2nd generation EHU. The 1st generation EHU uses an external gear machine coupled with an air-cooled permanent magnets electric machine; the 2nd generation EHU uses an internal gear machine integrated into a liquid-cooled permanent magnets electric machine. Both generations aim to a great level of components integration, power density and component reductions. To this extent the EMs are designed to host the HMs inside their rotor inner radius. Doing so, the designer can take advantage of the larger radius of the EM to develop more torque, while using a volume that would be otherwise nonfunctional. Such expedient allowed the EHU morphology to transition from a traditional arrangement where the EM and HM have different cases and are connected by a shaft, to the proposed arrangement shown in Figure 13.

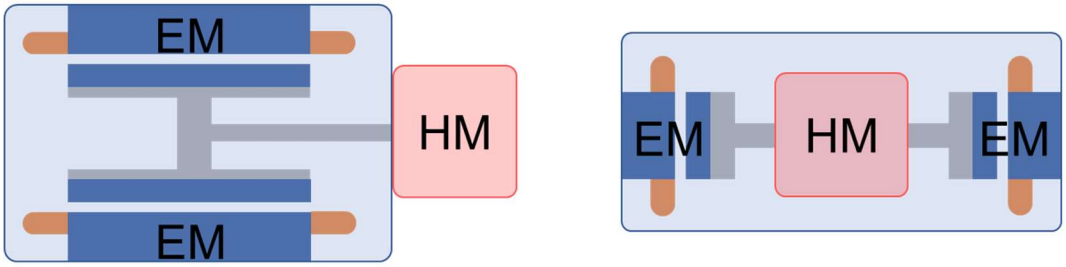

Figure 13: Left: traditional arrangement. Right: proposed arrangement.

Even if the two generations are very similar conceptually, they both have distinct features and presented their specific challenges. In the first budget period the 1st generation HM and EM are designed using an optimization procedure that embeds models already developed by the PI. Moreover, the morphology of the 2nd generation is thoroughly designed to accommodate the component reduction and the EM liquid-cooled system.

2.4 1st generation simulation models and optimization procedure

This paragraph describes the accomplishment of the milestone named "EGM EH-Unit Design Architecture Comlpeted".

In the first stage of the project the focus was on the design of the 1st generation EHU and on the definition of the morphology of the 2nd generation. The 1st generation EHU was designed combining two models. The first model is HYGESim (HYdraulic Gear machine Simulator). This

model was developed by Vacca's team in the last decade. As shown in Figure 14 such model is constituted by several sub-modules.

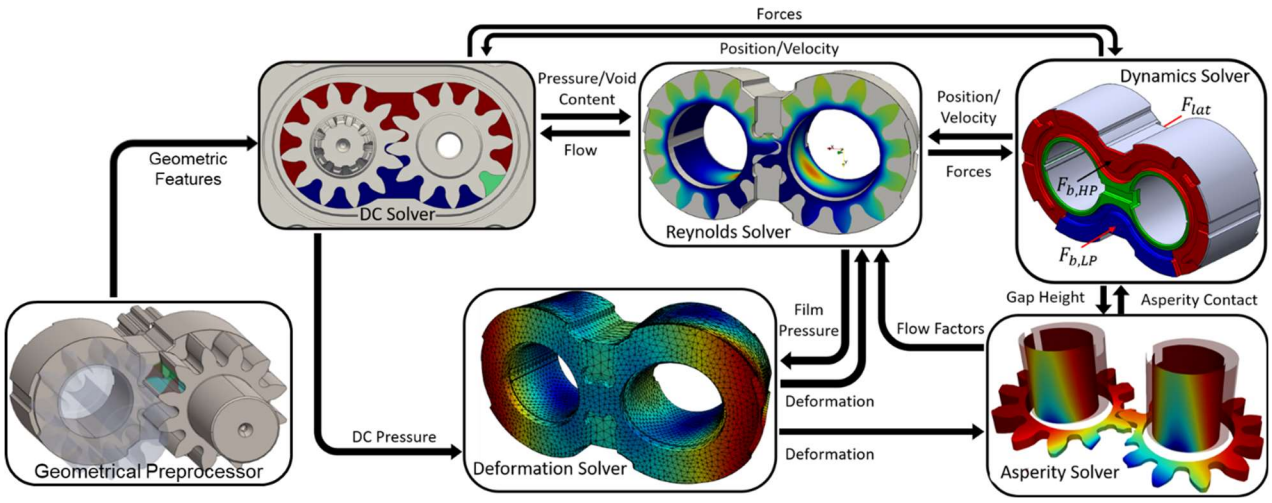

Figure 14: HYGESim simulation model conceptual schematic

Geometrical Preprocessor. In the geometrical preprocessor are input the parameters defining the gear set profile. After the gear set profile is defined the internal volume of the HM is partitioned in sub-volumes. There, many geometrical features such as the volume of the partitions and the connection areas between partitions are calculated. The calculations are repeated multiple times to generate a bidimensional look up table that report these geometrical features as a function of rotation angle and gear position.

DC Solver. In the displacement chamber (DC) solver, the information generated by the geometrical preprocessor are used to build the equivalent hydraulic circuit of the HM. The DC solver calculates the pressure in the internal sub-volumes of the HM and the flow established between them. In the DC Solver module, the forces generated by the hydrostatic pressure built in the partitions are calculated.

Reynolds Solver. The Reynolds solver provides a 2D solution for the flow and forces established inside the lubricating gaps at the gear lateral interface and at the shaft journal bearings. These gaps are key for determining the gap leakages and the shear forces on the rotating parts. The Reynolds equation in these gaps is solved also considering the hydrodynamic terms due to non-uniform gaps and film squeeze effects due to the motion of the bodies. A universal formulation of the Reynolds equation, based on the solution of the film density, allows to consider effects of aeration and vaporization.

Deformation Solver. The pressure field generated in the lubricated gaps is strongly affected by the gap morphology, which is highly dependent on the material deformation of the parts. For this reason, the model evaluates the material deformation through a pre-processed FEM based approach to determine the instantaneous body deformation using an influence matrix approach that allows speeding up the calculations.

Asperity solver. The parts in relative motion (i.e. the gears and the lateral bushings) can form gaps of a magnitude comparable to the surface finishing roughness. To account for the additional film pressure generation due to surface asperity, an average form of the Reynolds equation is utilized according to the theory first established by Patir and Cheng.

Dynamic Solver. In the dynamic solver the forces calculated in the DC Solver and the Reynolds Solver are used to solve Newton's second low and determine the position of the HM parts. With the newly calculated position of the gears, the HM internal geometrical features are updated, and the simulation proceed one timestep forward.

Even though such model allows very thorough simulation of the HM it requires a very long simulation time, which do not suit very well optimization procedures that aim to analyze 10^3-10^6. Therefore, the model reported above was simplified substituting the Reynolds Solver, Deformation Solver, Asperity Solver with the Mobility Solver for the journal bearing and considering a constant gap height for the lateral gaps. In the Mobility Solver the gears shafts are considered infinitely rigid, and the mobility method is used to calculate the reaction forces that bear the gears. Assuming constant lateral gap allows to have a reasonably accurate prediction of the volumetric losses with a fraction of the computation time that a CFD approach would require.

In Figure 15 is represented the conceptual schematic of the simplified model.

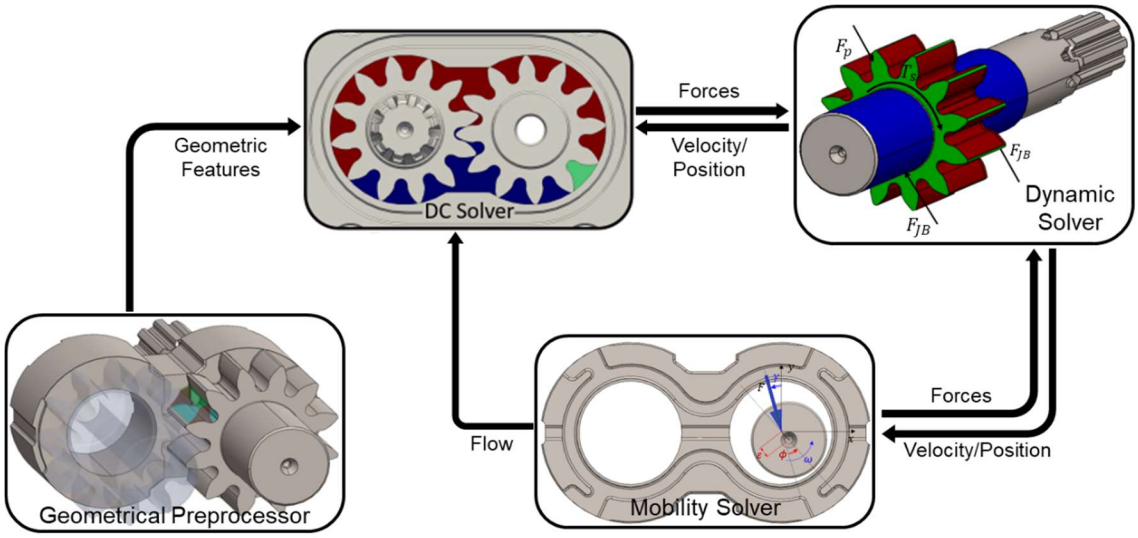

Figure 15: Simplified HYGESim simulation model conceptual schematic

To design the 1st generation EHU, HYGESim was coupled with a second model dedicated to the permanent magnets electric machine.

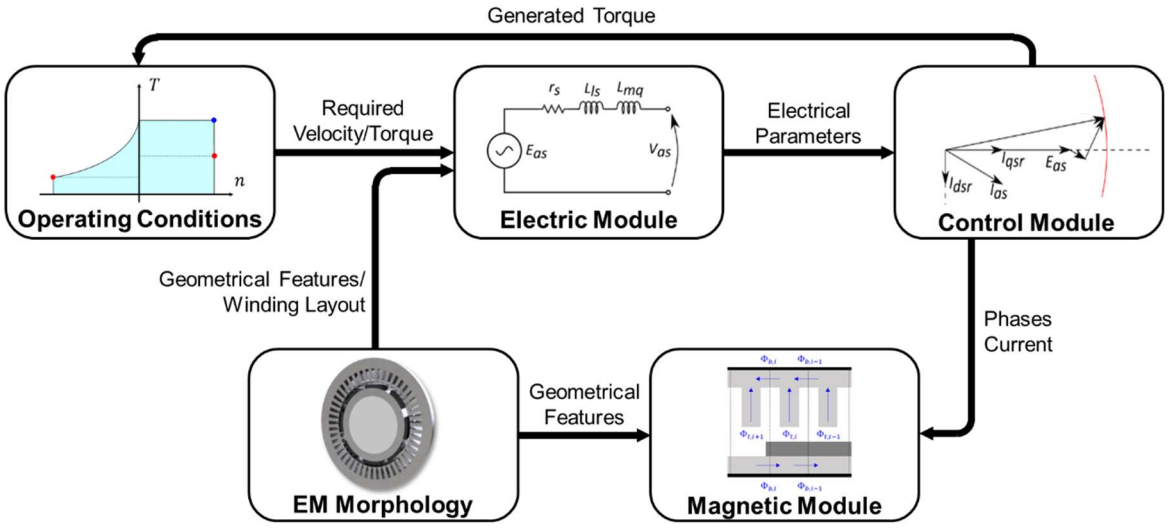

Figure 16: Permanent magnets electric machine model conceptual schematic

In the permanent magnet model the operating conditions and the EM morphology is defined. Then, a control low is imposed, and an electric and a magnetic analysis of the EM is performed.

The two models are coupled and embedded in the optimization procedure, which conceptual schematic is represented in Figure 17.

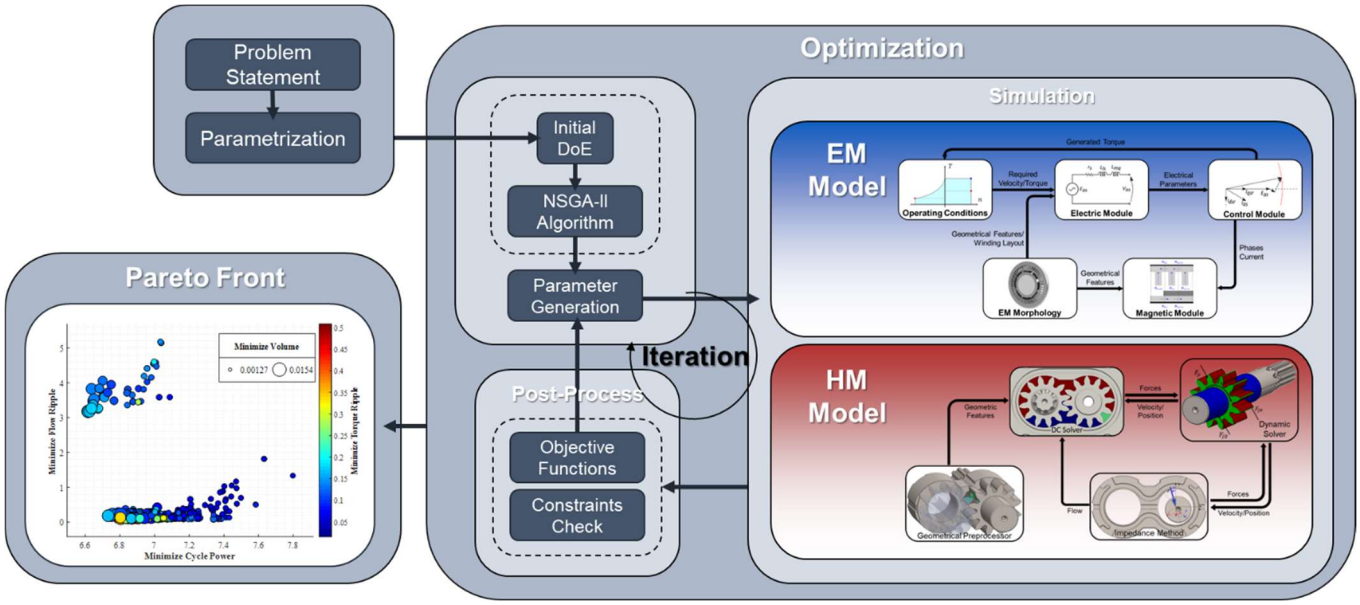

Figure 17: Optimization procedure schematic

2.4.1 Objective function

Coupling the two models is possible to simulate the EHU and evaluate its performance with respect to the objective function of the optimization.

Maximizing efficiency. The first objective function focuses on minimizing the power consumption on the duty cycle. To do so, a simplified duty cycle of the lift function of the actuator of the reference machine is considered. The simplified duty cycle is composed by a raising phase, where the EHU actively displace high pressure fluid in the actuator, and a lowering phase, where the EHU function as generator allowing the recuperation of energy. In Figure 18 the simplified duty cycle is represented, in red is highlighted the raising phase of the actuator and in green the lowering phase of the actuator. Each of these two phases is characterized by a specific rotation velocity and applied differential pressure, which are the operating conditions simulated to calculate the total efficiency of the EHU.

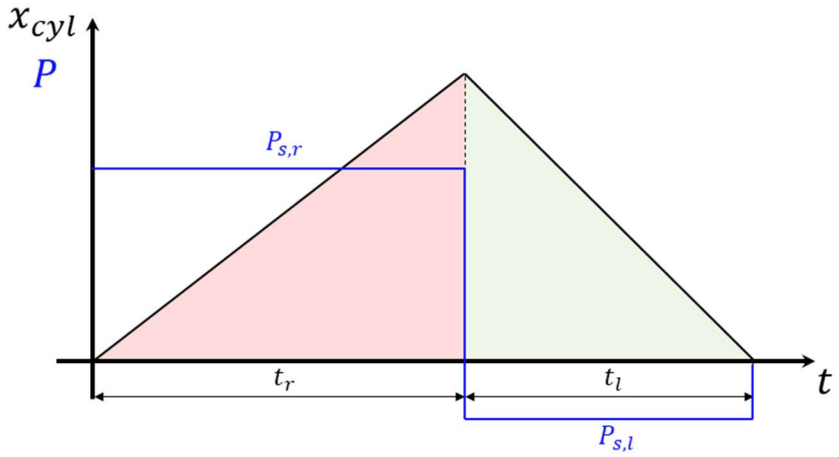

Figure 18: Simplified duty-cycle diagram

Minimize torque and flow ripple. To reduce noise and vibration the power level of the flow and torque ripple signal are analyzed and minimized. In addition to the operating condition constituting the duty cycle it is evaluated also the corner point operating condition.

To evaluate the efficiency and the functionality of the EHU each design must undergo through the simulation of the two operating conditions constituting the nominal duty cycle and the pumping mode peak power operating conditions. The three operating conditions are reported in

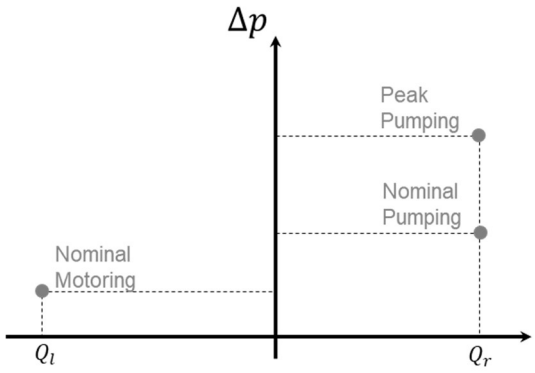

Figure 19: Representation of the analyzed operating conditions

Minimizing the volume. To ease the integration of the EHU on any commercial vehicle its total volume is minimized.

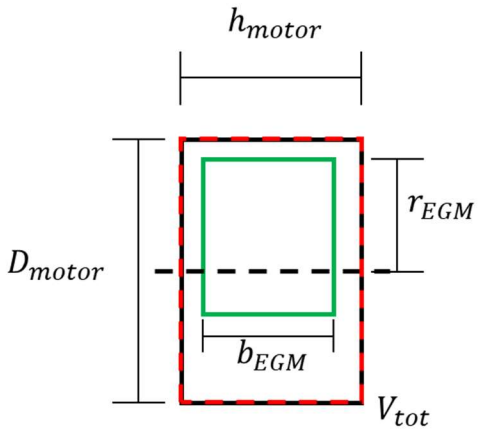

Figure 20: Conceptual schematic of the 1st generation EHU used to calculate the total volume

2.4.2 Constraints

To ensure the generation of properly functioning designs some constraints are imposed. First, the mean fluid inlet velocity is calculated and limited to a value that ensure the proper filling of the HM. Additionally, two constraints are imposed on the tooth space volume (TSV) pressure profile. The TSV is the volume between teeth of a gear machine, highlighted in Figure 21.

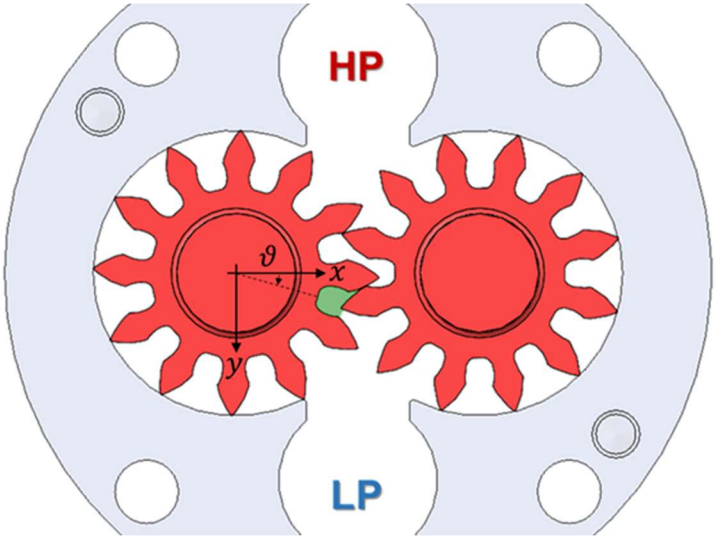

Figure 21: HM 3D model with TSV highlighted in green

The meshing zone of positive displacement gear machines is critical and must be properly designed. More precisely, to transition from the high-pressure region to the low-pressure region the TSVs must allow a minimal connection between the two. However, if the minimal connection is not realized, undesired phenomena like the generation of pressure peak can arise. To avoid the generation of pressure peak a constraint is imposed. Second, to limit the localized cavitation that

may happen after the meshing zone, a constraint is imposed on the cavitation area. The cavitation area is the area identified by the TSV pressure profile and the inlet pressure when the TSV pressure is below the inlet pressure. When the TSV pressure goes below the inlet pressure the gas in the fluid is released and the bubbles that can prevent the complete filling of the HM are formed. This area is a useful index of how much a gear set will tent to cavitate and its calculation is not computationally expensive. Both the pressure peak generated in the meshing zone and the cavitation area are highlighted in figure Figure 22.

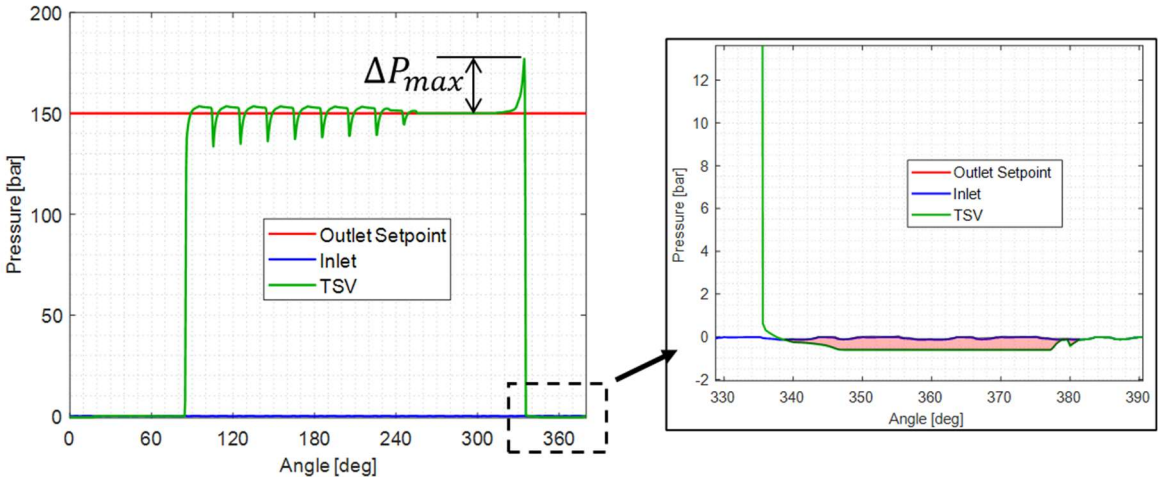

Figure 22: Tooth space volume pressure profile with highlights of cavitation area and pressure peak generated in the meshing zone

2.4.3 Results

The optimization process described in the above sections produced the pareto front from which a design is selected.

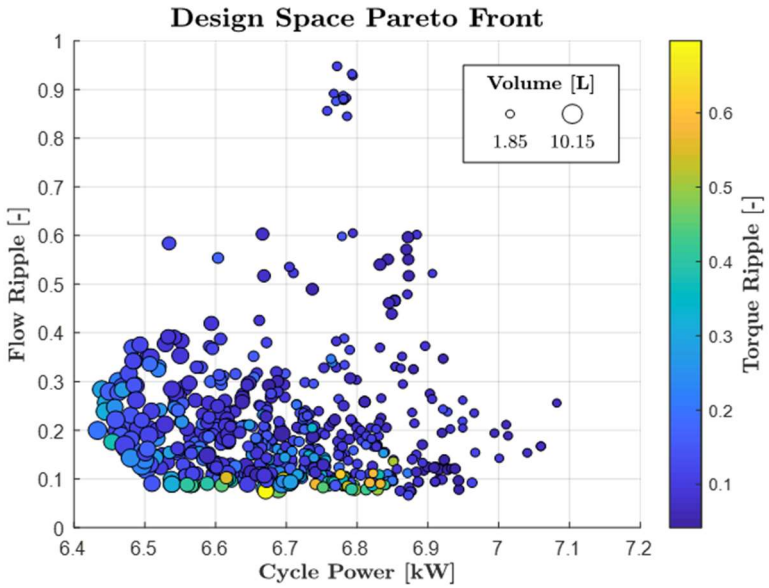

Figure 23: Optimization procedure pareto front.

For completeness, the HM gearset and EM parameters are reported in the table below.

HM Parameter		**EM Parameters**	
No. of teeth [-]	12	Rotor lamination material	M15
Th. displacement [cc/rev]	10.69	Stator lamination material	M15
Module [mm]	2.35	Perm. magnets material	Sm2Co17-R30S
Addendum [mm]	3.15	Conductor material	Copper
Dedendum [mm]	4.14	Pole pairs [-]	6
Drive pressure angle [deg]	14.9	Depth of inert region [mm]	60
Cost pressure angle [deg]	10.84	Depth of rotor back iron [mm]	7.53
Drive root radius of curvature [mm]	0.005	Magnets depth [mm]	3.02
Cost root radius of curvature [mm]	0.329	Air gap [mm]	1.50
Profile correction [mm]	0.31	Depth of tooth base [mm]	12.57
Gear width [mm]	20.11	Tooth fraction [-]	0.55
Nominal interaxis [mm]	30.69	Depth of stator back iron [mm]	7.83
Helix angle [deg]	0	Permanent magnets fraction [-]	0.7
Journal bearing shaft length [mm]	8.03	Active length [mm]	61.08
Journal bearing shaft diameter [mm]	10.71	Peak found. cond. dens. [cond/rad]	39.75
Journal bearing radial clearance [μm]	20	Coeff. of 3rd harmonic cond. dens.	0.34
HP relief groove-int. distance [mm]	1.64		
HP relief groove angle [deg]	25.46		
LP relief groove-int. distance [mm]	2.12		
LP relief groove angle [deg]	25.98		

Table 4 – Parameters of selected EHU design

At this stage of the design only the gearset and the EM are defined (Figure 24), however, to minimize the volumetric losses the axial compensation system must be carefully designed.

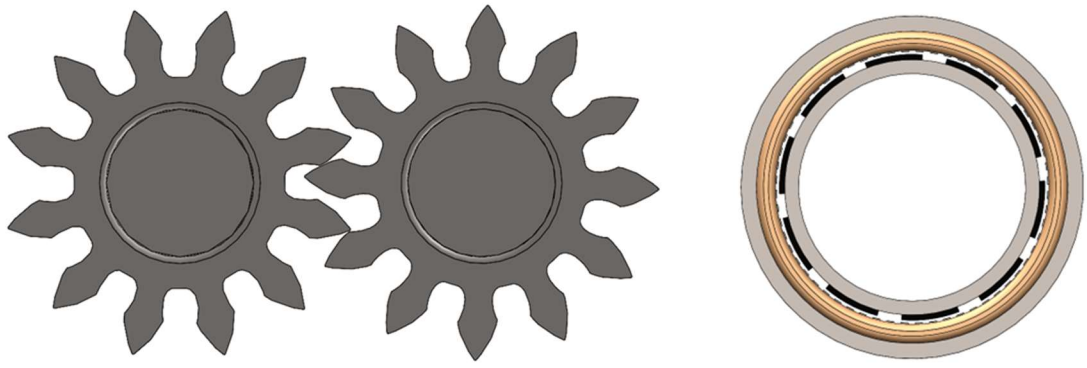

Figure 24: Selected EHU gearset and EM

2.4.4 Axial compensation system design

To design the axial compensation system all the modules of HYGESim are used, therefore, the pressure field generated in the lubricated gap is calculated solving the Reynolds equation with a CFD approach accounting for deformation and surface roughness of the plates. In Figure 25 is possible to see a representation of the TSVs pressure and a representation of the hydrodynamic

pressure generated in the lubricated gaps between gears and axial compensation system. These two axial actions act on the lateral plates producing their deformation, also highlighted in Figure 25.

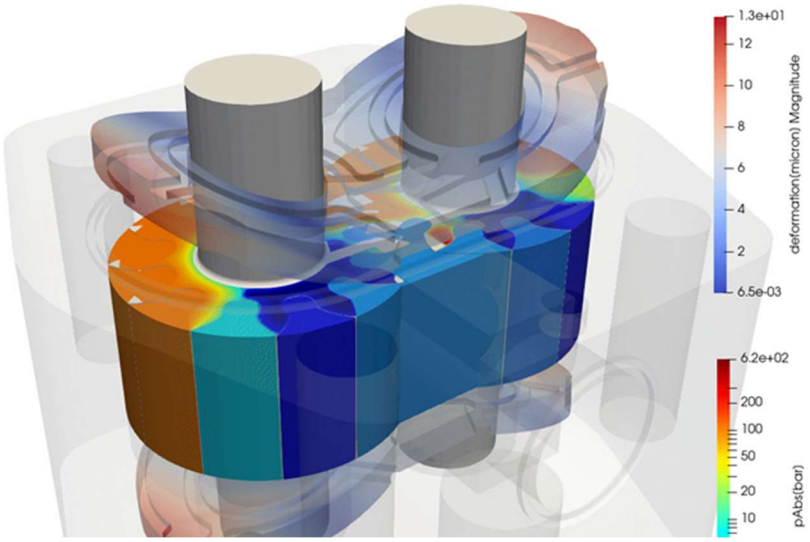

Figure 25: Image representing the pressure built in the TSV and the lubricated gap. The lateral plates are presented in their deformed configuration.

2.5 2nd generation morphology definition

This paragraph describes the accomplishment of the milestone named "4-Quadrant Hydraulic Architecture Completed".

The 2nd generation EHU uses an internal gear machine and the EM is liquid cooled. To put in place these modifications the design process first focused on defining a morphology that could host such solution achieving the greatest compactness and reduction of components. To evaluate all the possible morphological solutions in a qualitative way the Pugh chart system was used. The Pugh chart system consists of focusing on one aspect at the time, list all the possible solutions to address such aspect, and the grade them with respect to the most important criteria.

One example related to the 2nd generation EHU is offered by the selection of hydraulic machine typology in Figure 26. In this case, the HM typologies evaluated are external gear type, internal gear type, gerotor, vane type, and axial and radial piston type. To grade each HM typology, criteria as efficiency, cost, noise emission and flow pulsation are used. Additionally, to each criterion is associated a weight according to its importance for the designer. For example, the package-power density ratio is of paramount importance, while the development time is less important. From the score reported below each column of the chart is possible to see that the IGM results the best HM for the project application.

			External Gear Machine		Internal Gear Machine		Gerotor		Vane Machine		Axial Piston Machine		Radial Piston Machine	
1	Efficiency	2	3.0	6.0	3.0	6.0	2.0	4.0	3.0	6.0	4.0	8.0	4.0	8.0
2	Costs	3	3.0	9.0	2.0	6.0	2.0	6.0	3.0	9.0	1.0	3.0	1.0	3.0
3	Robustness	2	4.0	8.0	4.0	8.0	4.0	8.0	3.0	6.0	3.0	6.0	3.0	6.0
5	Noise emission	2	2.0	4.0	3.0	6.0	3.0	6.0	3.0	6.0	2.0	4.0	2.0	4.0
6	Flow Pulsation	1	3.0	3.0	4.0	4.0	4.0	4.0	3.0	3.0	3.0	3.0	3.0	3.0
7	Packaging-Power Dens.	3	3.0	9.0	4.0	12.0	4.0	12.0	3.0	9.0	3.0	9.0	2.0	6.0
8	Response Time	1	4.0	4.0	4.0	4.0	4.0	4.0	3.0	3.0	3.0	3.0	3.0	3.0
9	Development time	1	4.0	4.0	3.0	3.0	3.0	3.0	2.0	2.0	3.0	3.0	2.0	2.0
10				0.0		0.0		0.0		0.0		0.0		0.0
11				0.0		0.0		0.0		0.0		0.0		0.0
12				0.0		0.0		0.0		0.0		0.0		0.0
13				0.0		0.0		0.0		0.0		0.0		0.0
14				0.0		0.0		0.0		0.0		0.0		0.0
15				0.0		0.0		0.0		0.0		0.0		0.0
16				0.0		0.0		0.0		0.0		0.0		0.0
17				0.0		0.0		0.0		0.0		0.0		0.0
18				0.0		0.0		0.0		0.0		0.0		0.0
19				0.0		0.0		0.0		0.0		0.0		0.0
20				0.0		0.0		0.0		0.0		0.0		0.0
		52		47.0		49.0		47.0		44.0		39.0		35.0
				0.90		0.94		0.90		0.85		0.75		0.67

Figure 26: Pugh chart developed to select the hydraulic machine typology used in the 2nd generation EHU.

The use of Pugh charts can be very helpful even to address less important features, such as the material used for a certain component, or the type of valve block used (Figure 27).

			Case-Endplate With Integrated Manifold		Customized Organic Valve-Block		Standard Manifold		Sandwich Plates	
1	Cost	3	1.0	3.0	2.0	6.0	3.0	9.0	4.0	12.0
2	Modularity	3	1.0	3.0	2.0	6.0	3.0	9.0	4.0	12.0
3	Compactness	3	4.0	12.0	3.0	9.0	1.0	3.0	1.0	3.0
4	Weight	1	4.0	4.0	3.0	3.0	2.0	2.0	1.0	1.0
5	Complexity	2	4.0	8.0	4.0	8.0	4.0	8.0	1.0	2.0
6	Robustness	3	4.0	12.0	4.0	12.0	3.0	9.0	3.0	9.0
7	High Scale Production	2	3.0	6.0	2.0	4.0	2.0	4.0	2.0	4.0
8				0.0		0.0		0.0		0.0
9				0.0		0.0		0.0		0.0
10				0.0		0.0		0.0		0.0
11				0.0		0.0		0.0		0.0
12				0.0		0.0		0.0		0.0
13				0.0		0.0		0.0		0.0
14				0.0		0.0		0.0		0.0
15				0.0		0.0		0.0		0.0
16				0.0		0.0		0.0		0.0
17				0.0		0.0		0.0		0.0
18				0.0		0.0		0.0		0.0
19				0.0		0.0		0.0		0.0
		60		48.0		48.0		44.0		43.0
				0.80		0.80		0.92		0.90

Figure 27: Pugh chart developed to select the type of valve block used in the 2nd generation EHU

For the sake of brevity, it is reported the choice tree developed in the design process where all the aspect, possible options, and selected solutions are highlighted. Since the dimension of the decision tree, it is reported in two levels that can be read from the left from the right. The two levels are connected through the dashed line, which for the upper level is at the far right, and for the lower level is on the far left.

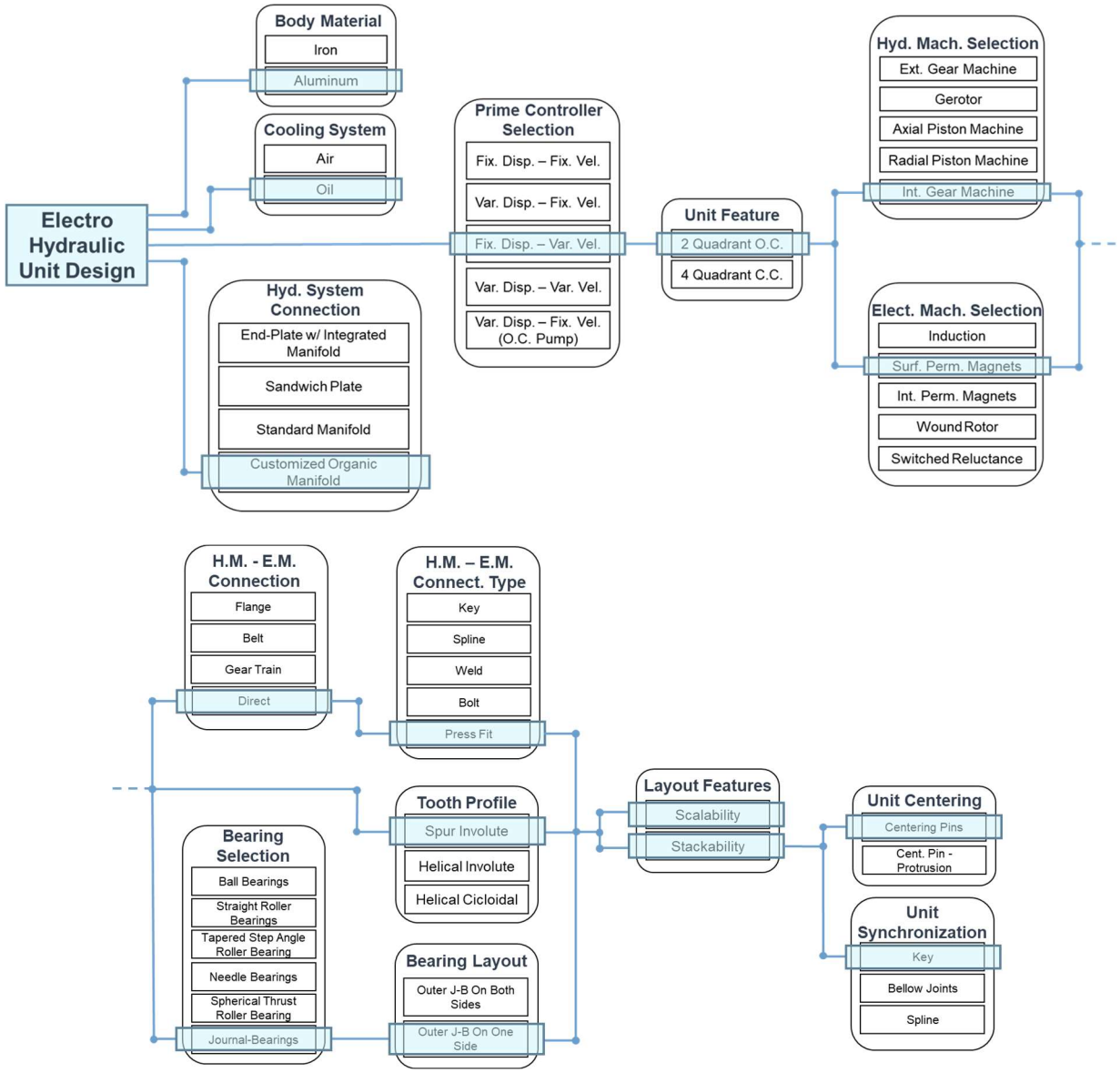

Figure 28: Decision tree generated during the design process.

3 Budget period 2

This chapter summarizes the work for the budget period 2 (BP2). Similar to the previous chapter, the contents are presented based on different technical milestones and GNG point.

3.1 EH module test & verification

To verify the functionality and performance of the proposed EH module, a dedicated test rig is built in Maha Fluid Power Research Center, Purdue University. Bosch Rexroth and CNH industrial support the hardware for the experimental setup.

Figure 29 shows the conceptual schematic of the test rig, which consists of two equal cylinders. One cylinder works as the actuator of the EH module, and the other one is the load drive, of which two reducing/relief valves are used to control the chamber pressure, so that a desired load

force can be applied. The cylinder has the same size of the boom actuator on the reference vehicle, so the test results are realistic prediction for the final technology demonstration on the vehicle.

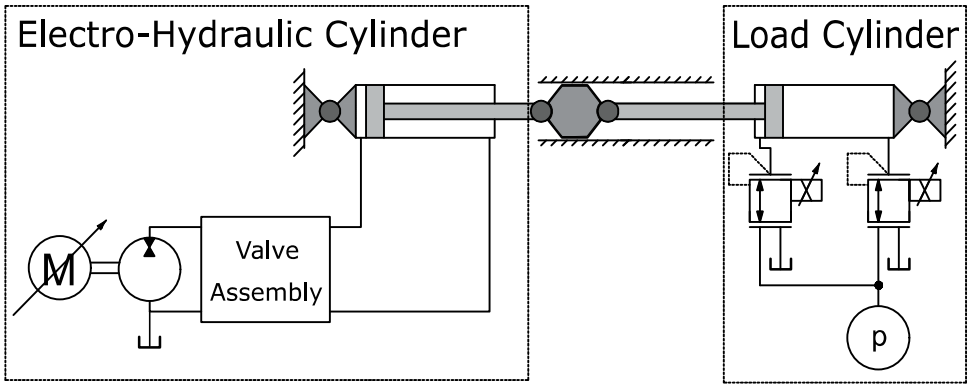

Figure 29: Conceptual schematic of the test rig structure

Figure 30 gives a picture of the experimental setup, the load drive and the EH module.

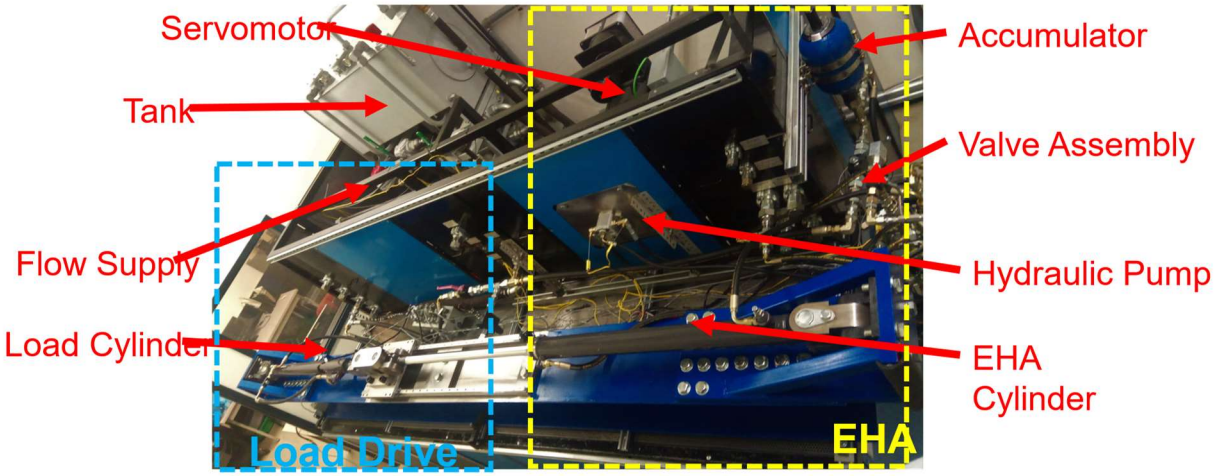

Figure 30: Picture of the test rig to verify the EH module

Figure 31 gives an example of EH module functionality validation regarding the speed control. The x-axis is the speed command, and the y-axis is the measured actuation velocity. The performance is linear with different loading force, in other words, the speed control strategy with pump and bypass valve is validated. Figure 32 shows the speed command, specifically the pump command. In the low-speed range and fast retraction mode, the pump speed is set at the minimum or maximum limit. However, the actuation speed can keep linear with the help of the bypass valve.

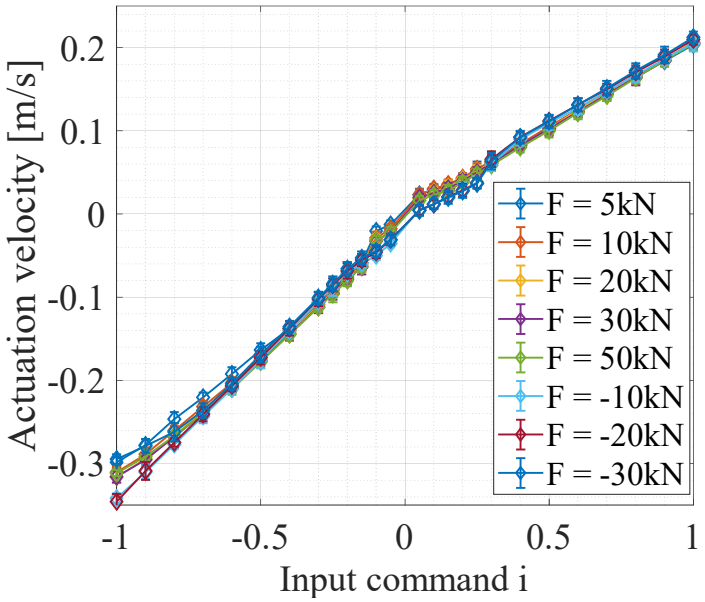

Figure 31: Speed control of the proposed EH actuation system

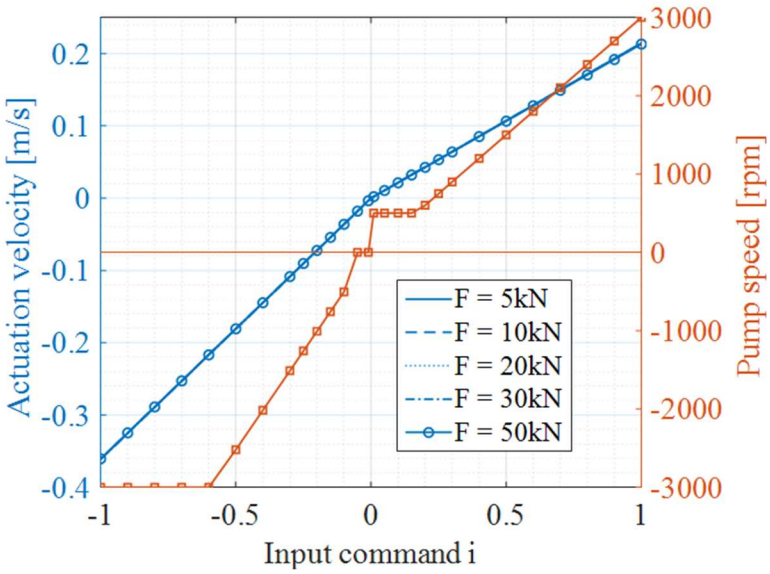

Figure 32: Speed command to the actuator and the pump

Figure 33 and Figure 34 show the efficiency maps measured from the test rig, for the open-circuit and closed-circuit layouts, respectively. The efficiency maps are in four-quadrant exclude the losses of electric machine, i.e., the map represents the hydraulic system efficiency.

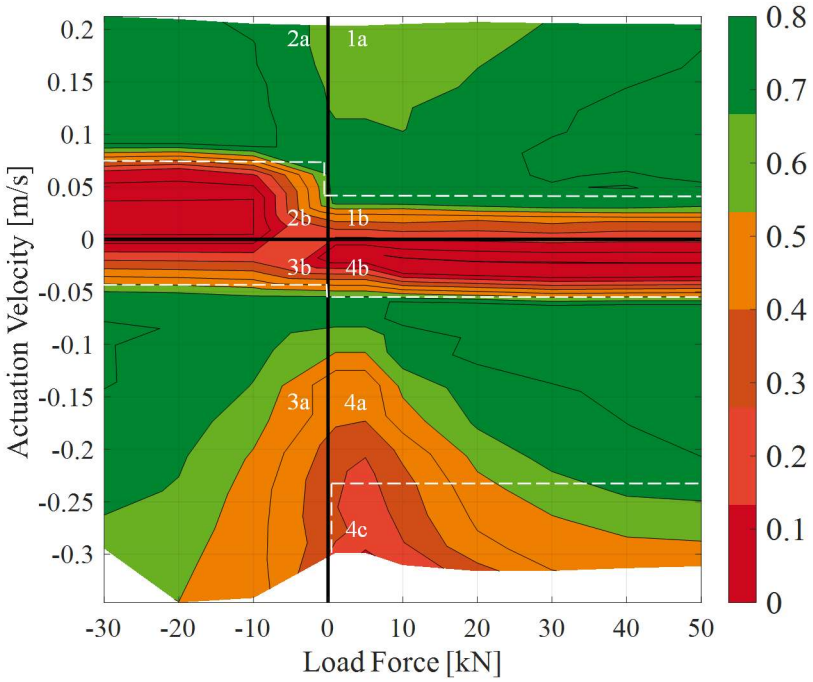

Figure 33: Measured efficiency map of open-circuit layout

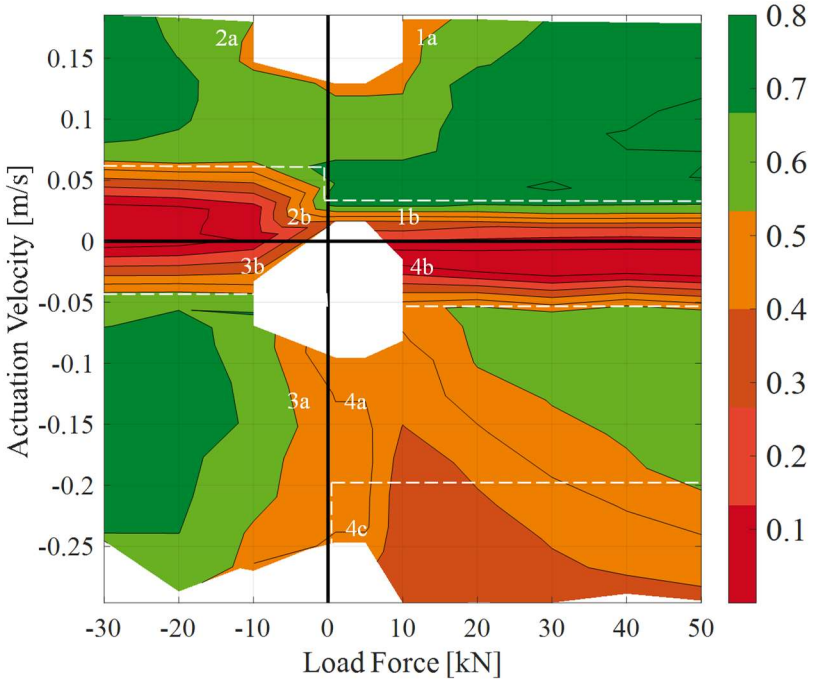

Figure 34: Measured efficiency map of closed-circuit layout

Both layouts have good efficiency performance up to 80%, which achieves the GNG milestone in BP2. In low-speed mode, as the bypass valve is used for speed regulation, more throttling losses are introduced and results in lower efficiency.

Comparing these two efficiency maps, the open-circuit layout performs better because of the more efficient behavior of the 2-quadrant hydraulic machine. Apart from the efficiency, a detailed study on the thermal behavior was conducted to both layouts, which showed that the self-contained open circuit EH module may have challenge on cooling, especially with aggressive/long duty cycles. Therefore, for the consideration of thermal management and efficiency performance, the open-circuit layout is selected as the solution for demonstration.

3.2 EH manufacturing and experimental test

This paragraph describes the accomplishment of the milestone named "4-Quadrant EH Unit Design Complete" and "4-Quadrant EH Unit Test".

While testing the EH module the parts of the 1st generation EHU are manufacture and assembled.

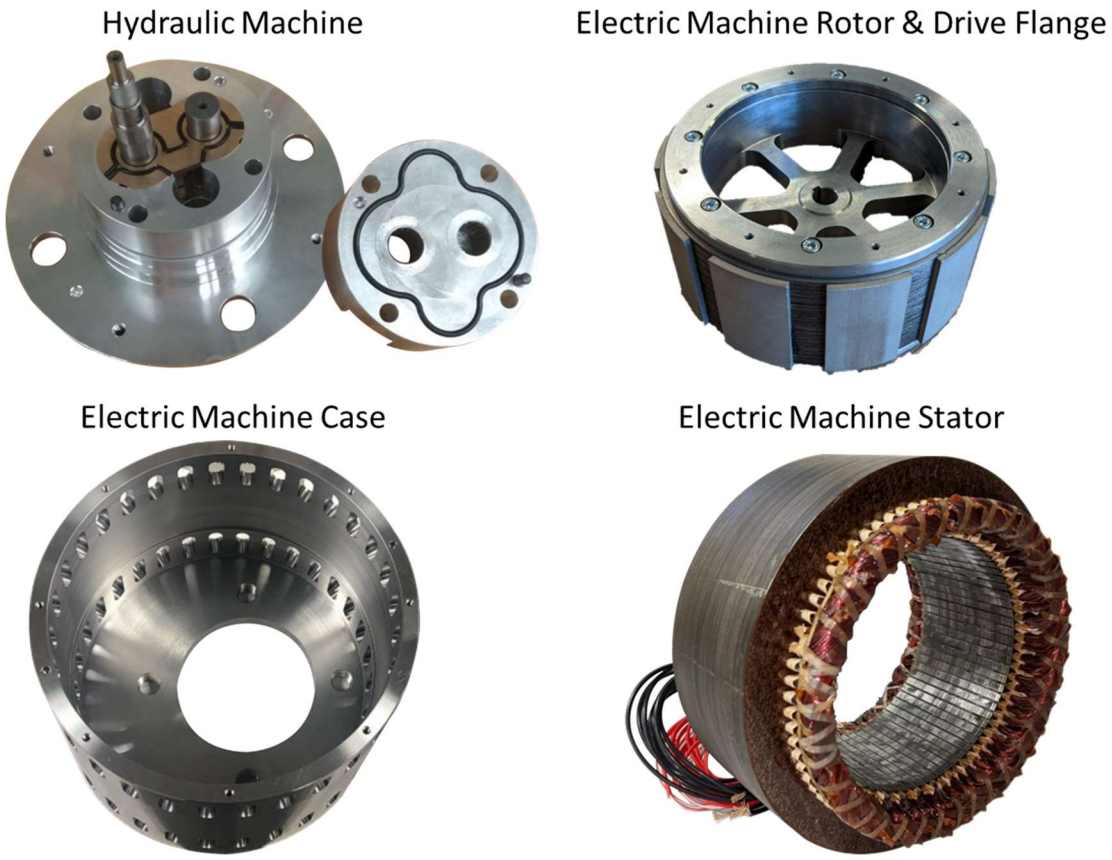

Figure 35: 1st generation EHU parts

In Figure 35 are reported the images of HM, EM casing, EM rotor and stator, which can be assembled with the other parts into the 1st generation EHU reported in

Figure 36: 1st generation EHU

After assembling the unit a dedicated hydraulic circuit is built to test its performance in terms of efficiency. The circuit with the sensors are reported in Figure 37. A pressure sensor and a temperature sensor are positioned at the inlet and outlet port of the EHU; in front of the outlet of the EHU is connected a filter, a flowmeter, and the load orifice in parallel with a relief valve for safety reason.

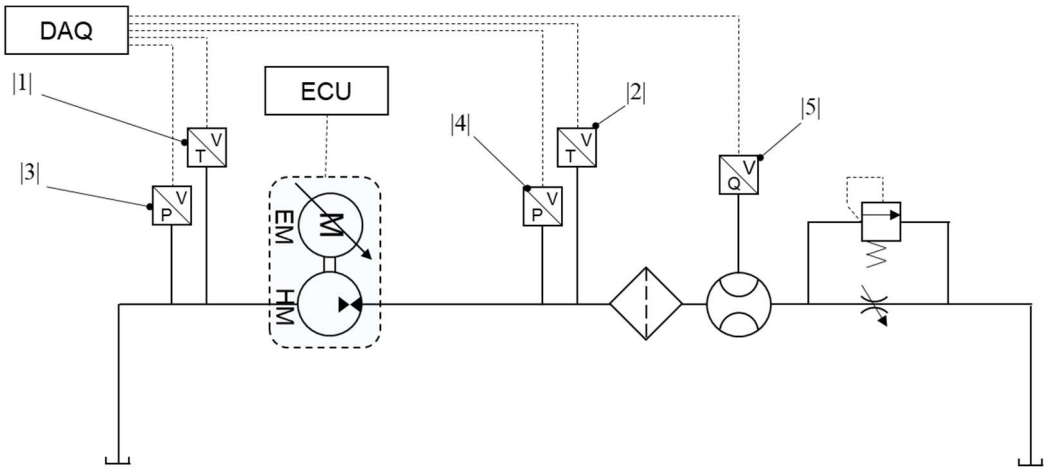

Figure 37: Hydraulic circuit dedicated to the test of the 1st generation EHU

For completeness, the sensors, and their accuracy are reported in Tab. 5.

	Sensor	Model	Specifications	Accuracy
|1|	Thermocouple K	Omega K-type	-5 to 200°C	1 °C
|2|	Thermocouple K	Omega K-type	-5 to 200°C	1 °C
|3|	Pressure Transducer	Keller Valueline	0-10 bar	±0.1% F.S.
|4|	Pressure Transducer	Hydac series 23	0-6000 psi	±0.5 % F.S.
|5|	Flow meter	VSE VS02	0.1-120 L/min	±0.3%

Table 5: Sensors used in the hydraulic circuit used to measure the EHU-

It is important to note that the EM of the EHU is powered with the inverter designed for this project.

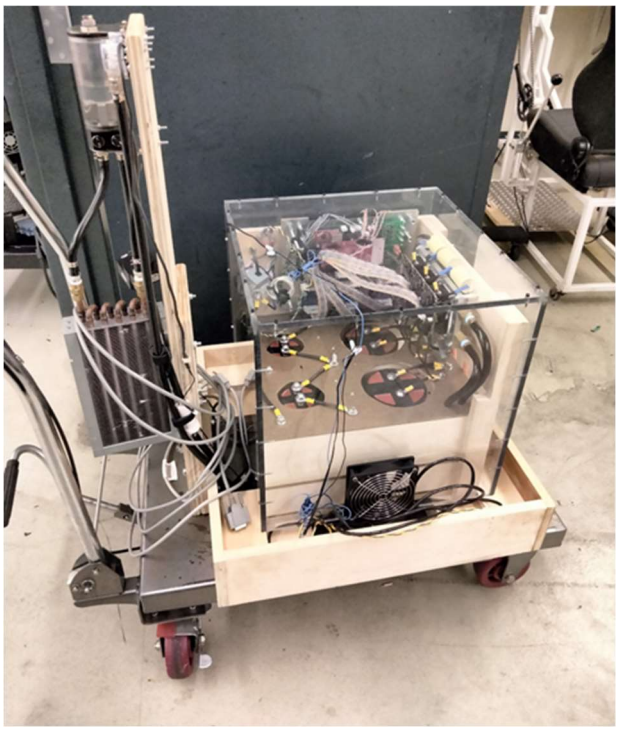

Figure 38: Inverter prototype

With the circuit reported in Figure 37 the EHU is tested and the results in Figure 39 and Figure 40.

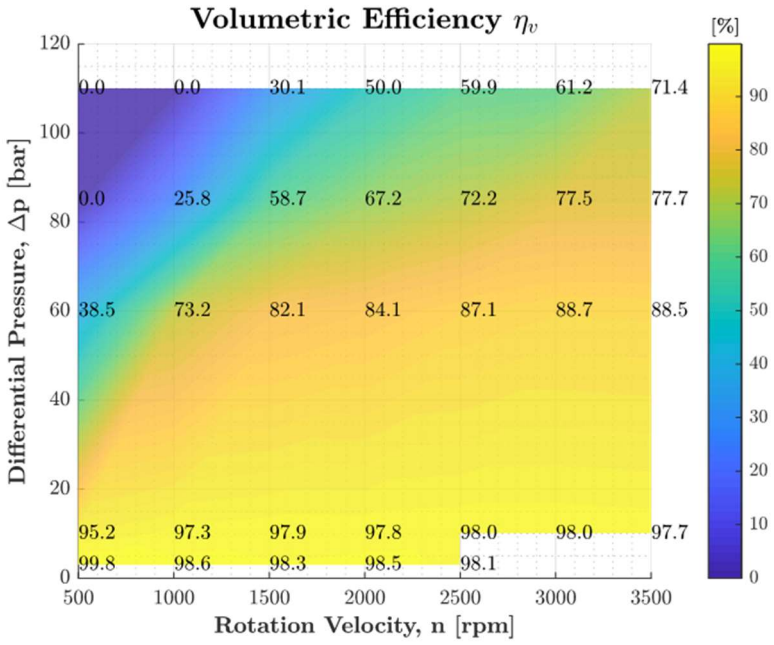

Figure 39: 1st generation EHU volumetric efficiency

Looking at the volumetric efficiency plot is possible to see that in the region of operating conditions characterized by low rotation velocity and high differential pressure the volumetric efficiency is null. That value corresponds to the impossibility of displacing fluid. This happens because of the loose tolerances imposed on the parts and the failure of axial compensation system seals which are handcrafted. Both these factors were dictated by the supply difficulties due to world pandemic of COVID-19.

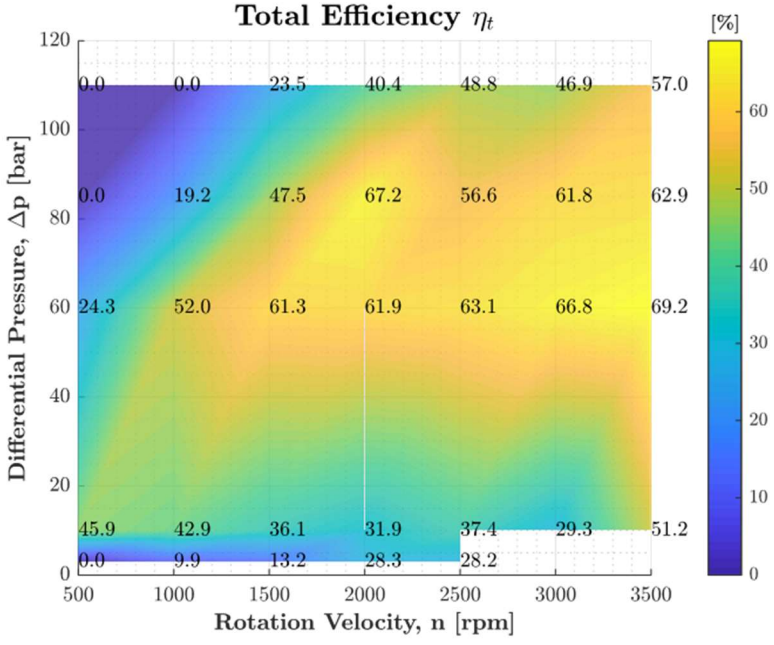

Figure 40: 1st generation EHU total efficiency

Analyzing the total efficiency results is possible to see that it is highly affected by the volumetric losses highlighted in the previous paragraph.

3.3 EH module demo with EH unit

This paragraph describes the accomplishment of the milestone named "Demo vehicle test" and "Quadrant EH Unit Demo and Vehicle Performance".

After the validation of the EH module functionality and the test of the EHU, the whole system with EH unit as the prime mover is further verified and demonstrated on the dedicated test rig. Figure 41 shows the picture of the test rig setup with the EHU installed.

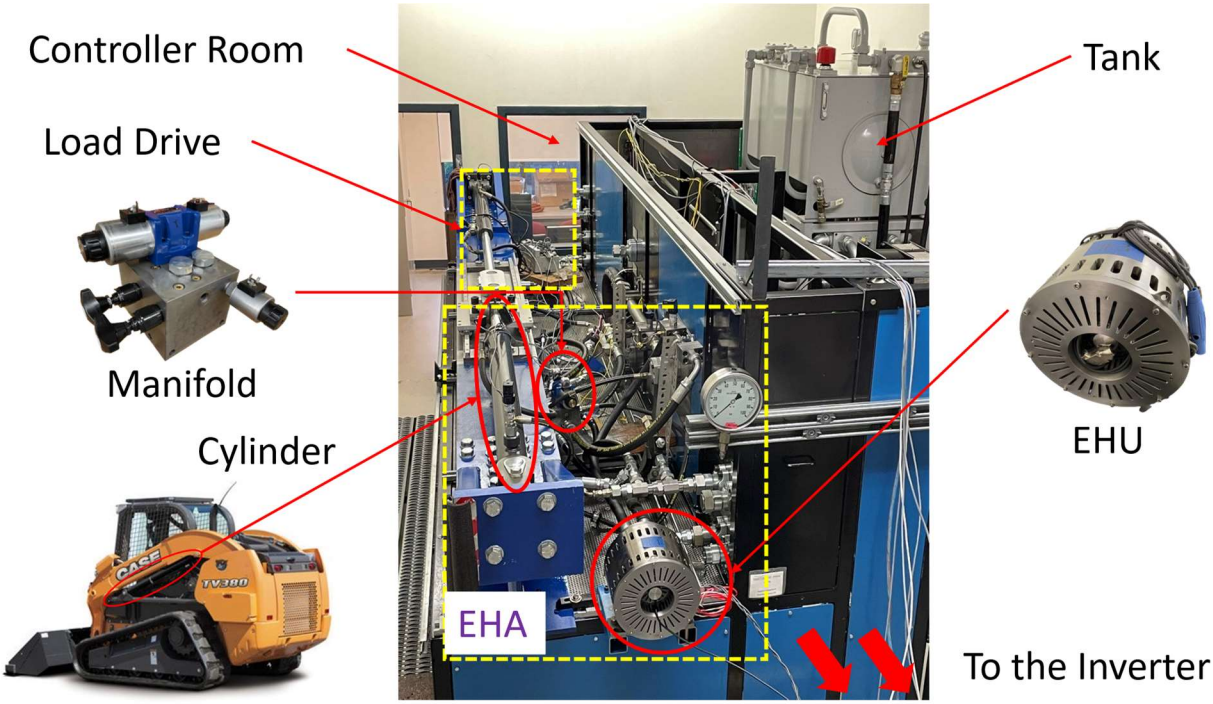

Figure 41: Picture of the test rig setup with the EH module and EH unit

The actuator has the same dimension with the one on the reference vehicle, boom function. Thus, the results obtained on the test reflect the real cycles, which is a good verification before the demonstration on the reference vehicle. Bosch Rexroth gave strong support on the hardware of the test rig and the power electronics setup (inverter and filters).

Figure 42 summarizes the results of the test rig demonstration. Four typical points are tested for the boom and bucket function, which also include all four-quadrant working modes. The overall efficiency of the EHA system is up to 54%, which is limited by the EHU prototype as of now. Further validation was conducted on the reference vehicle in the next chapter.

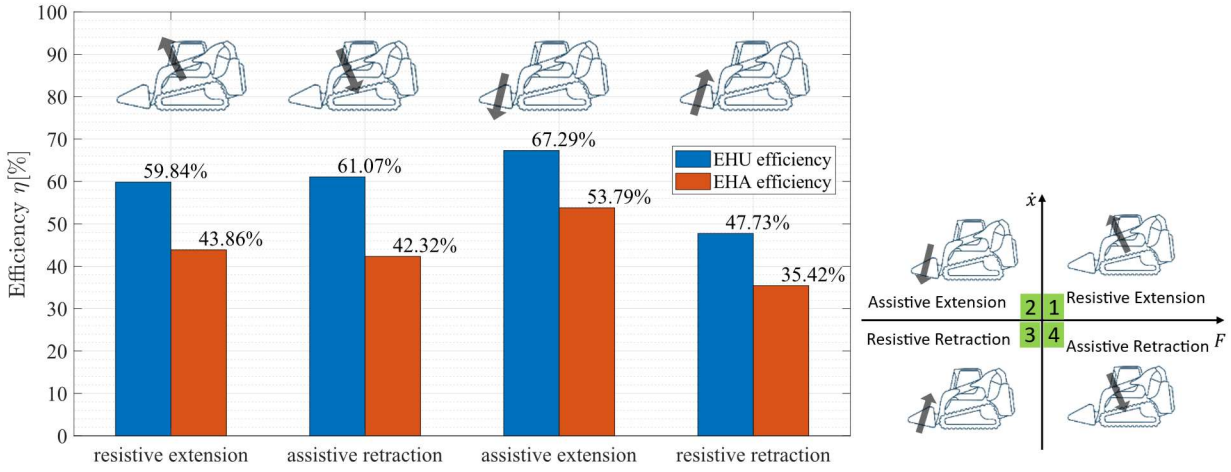

Figure 42: Efficiency performance in four-quadrant on test rig demonstration

Regarding the EHU efficiency performance, Table 6 summarizes the results from the test rig. Both the pump mode and motoring mode are included in the demonstration, and the overall efficiency is about 60%, which reach the target of GNG point in BP2.

Table 6: EH Unit performance measured on the test rig

	Pumping mode ($\boldsymbol{n = 3866rpm,\ p = 64.5bar}$)	**Motoring mode** ($\boldsymbol{n = -2901rpm,\ p = 37.1bar}$)
Volumetric efficiency $\boldsymbol{\eta_{vol}}$	76.1%	93.9%
Hydro-mechanical efficiency $\boldsymbol{\eta_{mech}}$	78.9%	65.0%
Overall efficiency $\boldsymbol{\eta_{EHU}}$	59.9%	61.1%

4 Budget period 3

This chapter summarizes the activities in budget period 3 (BP3), which are mainly about the implementation of the proposed EH system and the technology demonstration on the reference vehicle.

4.1 EH module implementation

This paragraph describes the accomplishment of the milestone named “EH Module Final Design”.

After the validation described in the last chapter, the EH module is finalized and ready for implementation. Figure 43 shows the final design of the EH module with a compact manifold, which is implemented in the EHA system with the EHU together. Bosch Rexroth supported to design and manufacture the valve manifold and EH unit.

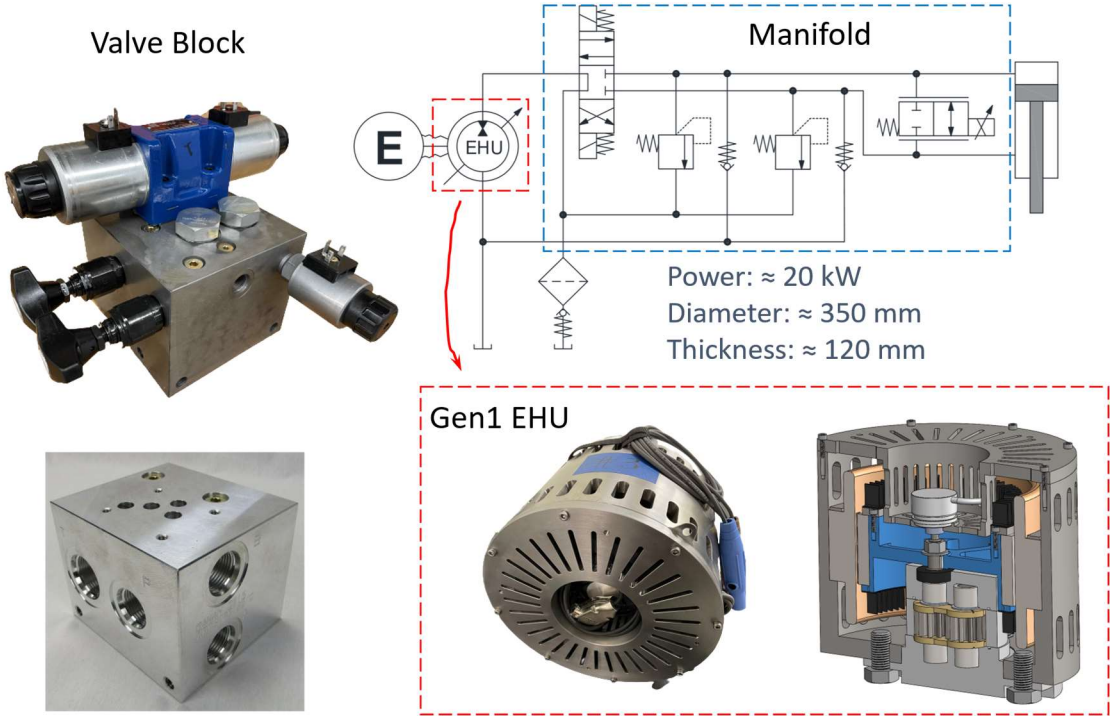

Figure 43: EH module final design and implementation

Figure 44 shows the overview of the experimental platform, including the power electronics, EHA drive, boom function of the reference machine, and the control and data acquisition system based on the Compact RIO. The speed control is achieved by the joystick command, like an operator on the reference machine.

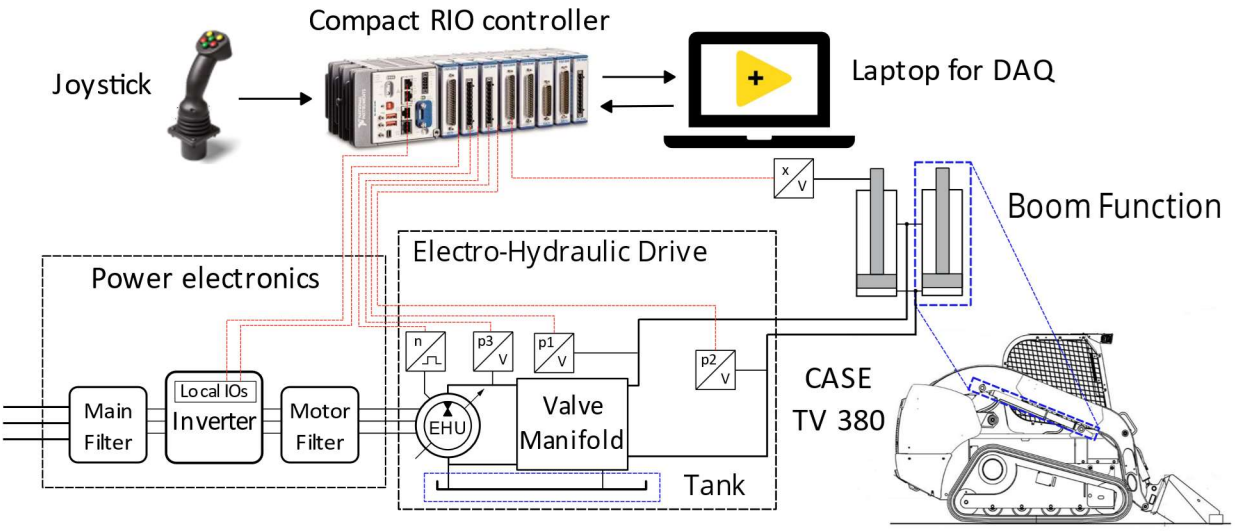

Figure 44: Overview of the experimental platform on the reference vehicle

Figure 45 gives a picture of the demonstration setup on the reference vehicle. The EH unit and EH module are installed at the back of the machine for an easy setup, which avoids the complex modification of the original powertrain of the reference vehicle. Two EHA systems are implemented to drive the boom and bucket actuators, respectively.

Figure 45: Demonstration on the reference vehicle, with two EHA systems to drive the boom and bucket functions

Figure 46 shows the hydraulic configuration of the boom function as an example.

Figure 46: Hydraulic configuration on the reference machine

The red arrows highlight the position of the hydraulic hoses between the EH module and the boom cylinder. T fittings are used to connect the boom cylinder to the EH module, so that no extra modifications are needed on the original hydraulic configuration. Either the EH drive or the open-center system on the machine can control boom function. The tank on the machine works as the reservoir of the EHA system.

4.2 Vehicle demonstration and performance

This paragraph describes the accomplishment of the milestone named "Demo Vehicle results".

Based on the set up detailed in Section 4.1, demonstration of the proposed EHA system with full four-quadrant functionality is conducted. The energy performance is analyzed based on the measured power flow and compared with the baseline.

Figure 47 shows the measurements for the EHA demonstration. The first plot represents the boom cycle in terms of cylinder displacement and velocity. The second plot highlighted with phase 1 and 2 shows the power. This time the system adopts electric power (DC bus) instead of engine power. The other two plots show the EHU speed, outlet pressure, and the loading force applied on the boom cylinder during the duty cycle.

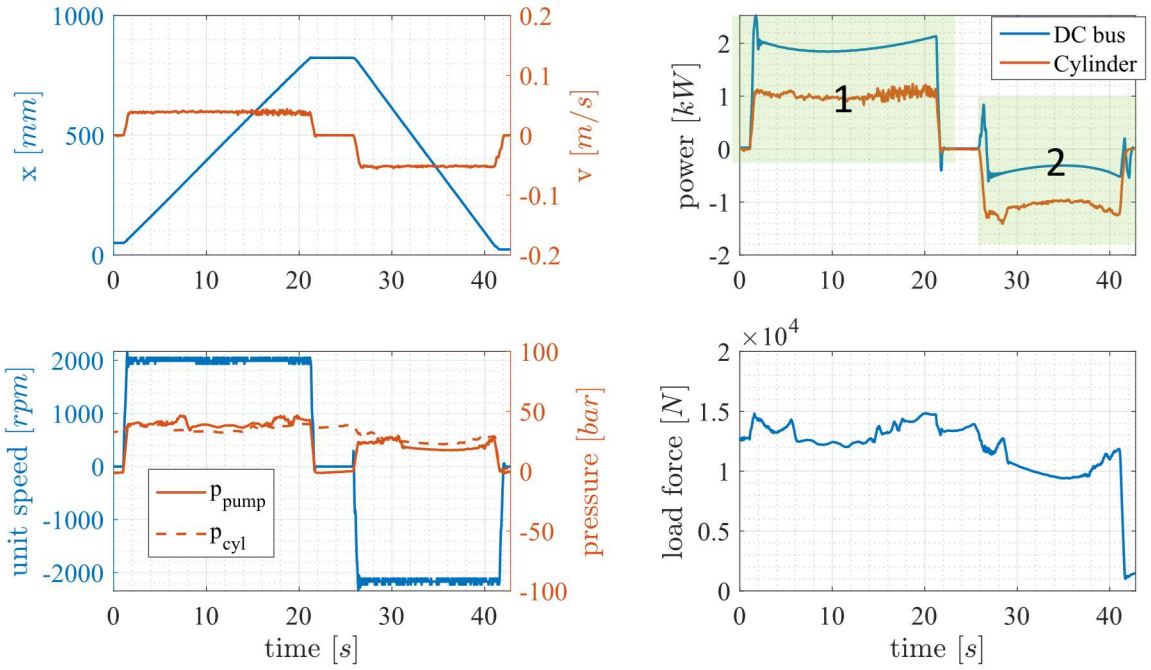

Figure 47: Measurements from the EHA demonstration, 50% speed

Focusing on the power plot, different from the baseline measurements, in phase 2 both the DC bus power and the actuator power is negative. This negative sign reflects the direction of the power flow, meaning the system is having energy regeneration.

Figure 48 is the energy flow scheme of the EHA, corresponding to the measurements given in Figure 47. In raising phase, the power electronics input power to the system, and the actuator works as the output. In lowering phase, the actuator inputs power from the boom gravity, and output power gets into the inverter side, as energy regeneration. If an energy storage device is installed, e.g., a battery, in this phase the battery can be charged by the energy from the boom lowering.

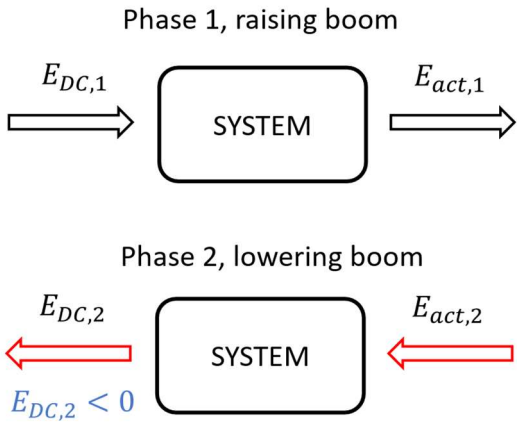

Figure 48: Energy flow scheme of the EHA demonstration with energy regeneration

With energy regeneration, (1) shows the definition of the efficiency in one cycle. The input and output energy change in phase 2, so the overall efficiency has enormous potential to improve.

$$\eta_{cyc} = \frac{E_{out}}{E_{in}} = \frac{E_{act,1} + |E_{DC,2}|}{E_{DC,1} + |E_{act,2}|} \quad (1)$$

Figure 49 shows the detailed power flow of the measurements given in Figure 47. The orange arrows give the power for resistive extension phase (raising boom), while the green arrows represent the assistive retraction (lowering boom). The numbers inside the arrows give the input/output power of each element in the system. Regarding the power losses, most come from the 1st Gen EHU prototype. The performance is expected to be improved after refurbishing the EHU components.

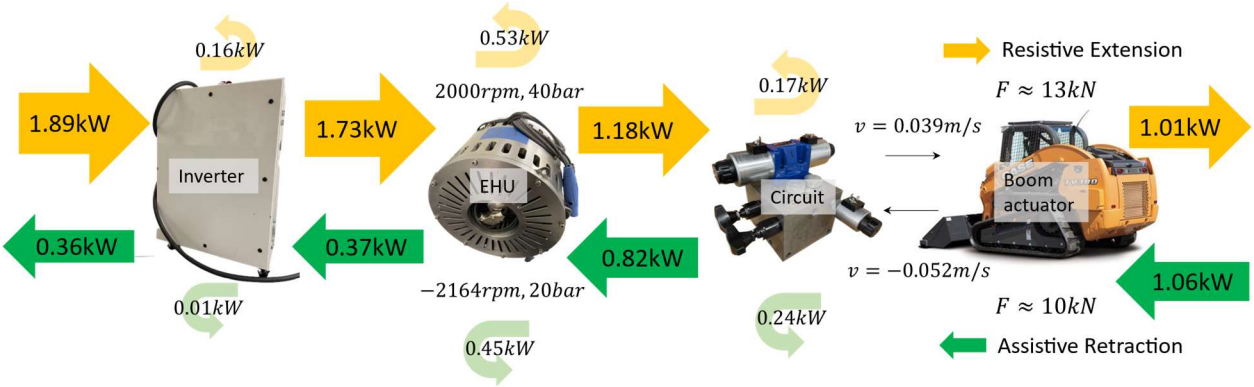

Figure 49: Power flow of the EHA demonstration with energy regeneration

Figure 50 gives a 'side by side' comparison of the EHA and the baseline system focusing on the power consumption. The duty cycles of these two measurements are similar, and the velocity of raising and lowering boom are remarkably close. As a result, the working conditions of the boom actuator are fairly the same, especially in terms of power in steady state, even there are some phase differences, such as the raising starting point, etc.

With a similar output power of the actuator, the input power shows obvious difference. In the lower plot, the orange curve is the engine power from the baseline, and the blue curve is the DC bus power, which is the input of the EHA system. The difference between the two curves highlighted in green is the energy saving. In raising phase, the EHA benefits from better efficiency. In lower phase, the energy saving comes from regeneration mode of EHA. Furthermore, in idle phase, the baseline needs to maintain a certain engine speed, resulting in more energy losses. Instead, for the electrified system, the idle power of the power electronics is zero. This 'idle saving' is another advantage of electrification, as in real duty cycles of applications, the power consumption from the idle engine plays a significant role. However, as the period of idle phase depends on application conditions, in this report the saving from the idle phase is not included in the analysis, and the focus is on raising and lowering cycle.

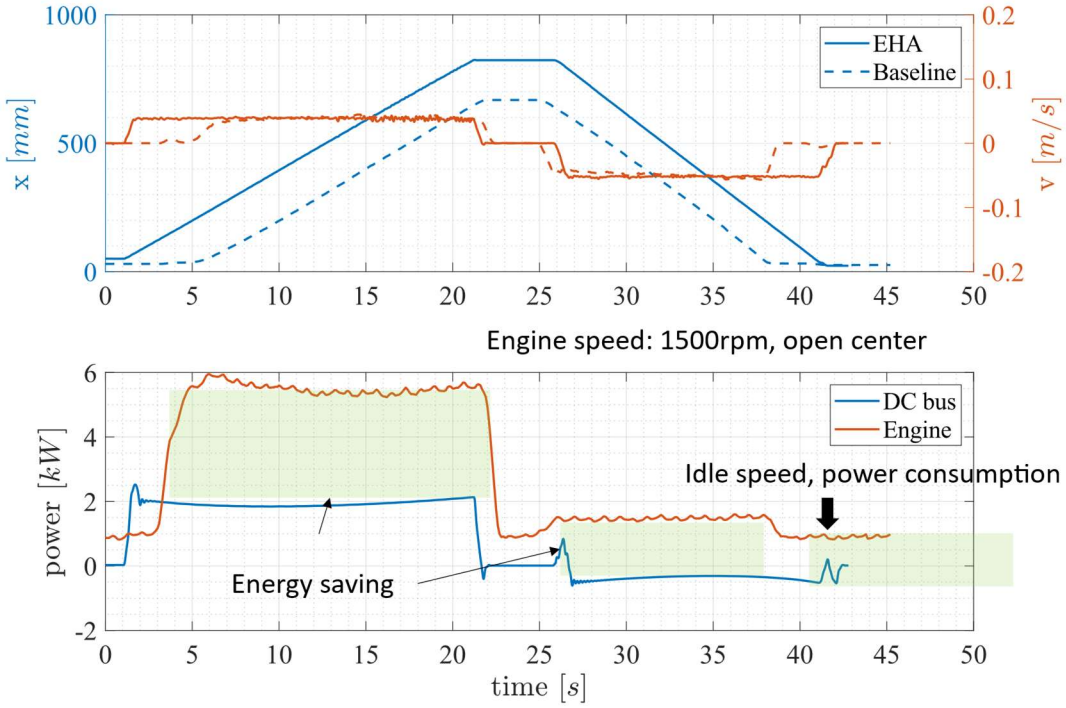

Figure 50: Comparison of EHA and baseline system, big saving

Regarding the efficiency in cycle defined in (1), Figure 51 gives a comparison of the EHA and the baseline. The bubbles at the bottom represent the baseline performance, where the orange ones show the metering control cases (normal operation of baseline), and the red ones show the operation with fully open valves (best efficiency of baseline). The blue diamonds are the performance of the EHA demonstration.

The proposed EHA improves the efficiency in cycle for all working conditions. When the baseline uses metering control, the improvement is more than 150%. And when the baseline achieves the best efficiency, with its minimum throttling losses, the improvement is still more than 30%. This impressive efficiency improvement achieves the target of BP3.

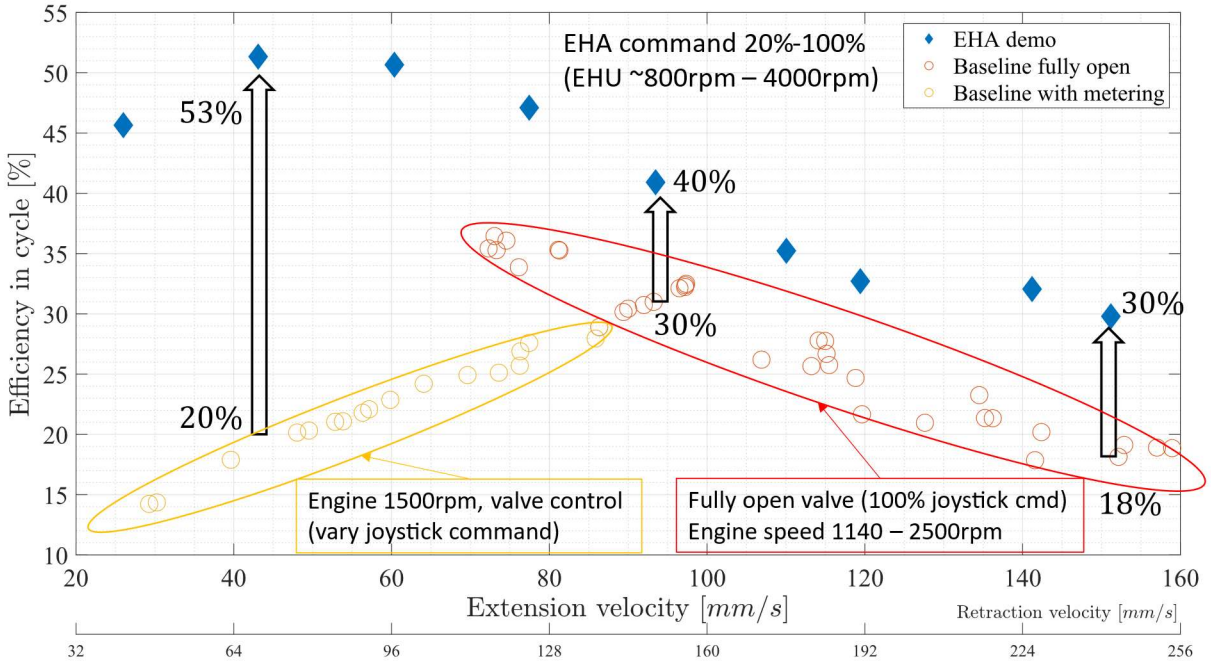

Figure 51: Improvement of efficiency in cycle, EHA vs baseline

Other than the improvement of efficiency performance, Figure 52 summarizes the energy consumption results with different speed for one duty cycle. Roughly, the EHA consumes only 1/3 energy for one duty cycle of the baseline in most cases. The input energy saving is based on the comparison between mechanical power to the pump for the baseline, and the electric power to the inverter for the proposed EH system. The fuel saving capability can be further studied on the energy source of the system.

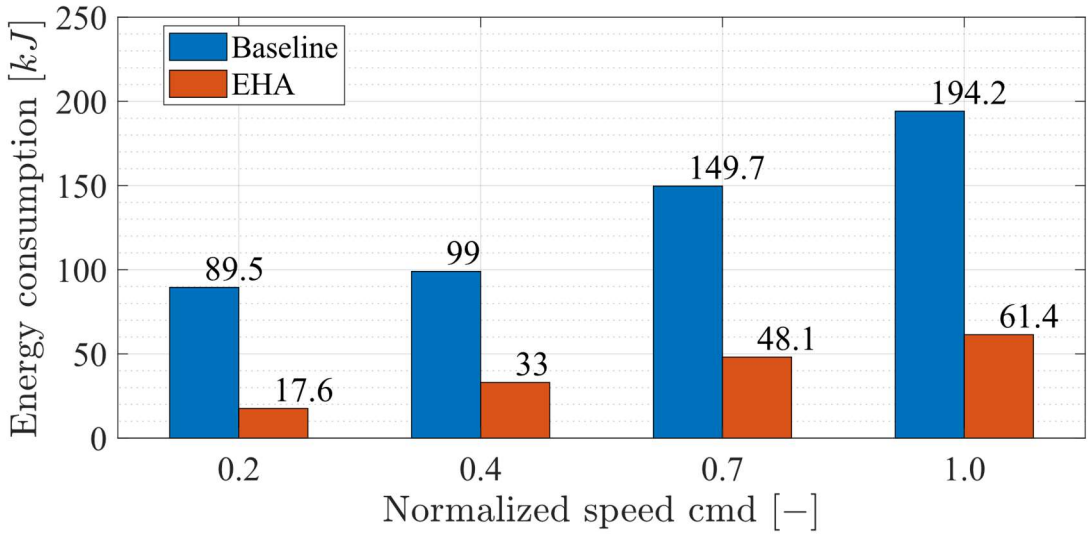

Figure 52: Energy consumption in one duty cycle, from low speed to high speed

Focusing on the performance of the Gen1 EHU, Figure 53 summarizes the efficiencies of the unit in the demonstration with different working conditions, including the volumetric efficiency in

the first plot, torque efficiency in the second plot, and the overall efficiency if the unit at the bottom plot.

With empty load and different speed, the pressure difference varies with a clear trend due to the friction of the mechanism and the pressure drop in the hydraulic circuit. This efficiency map expands to two-quadrant and includes the regeneration mode with negative speed. When the differential pressure is low, the EHU may not regenerate energy, so the torque efficiency is zero. This phenomenon is also shown in Figure 53**Error! Reference source not found.**. In brief, the overall efficiency of the Gen1 EHU varies from 60% to 70%, which also validates the measurements on the test rig shown before.

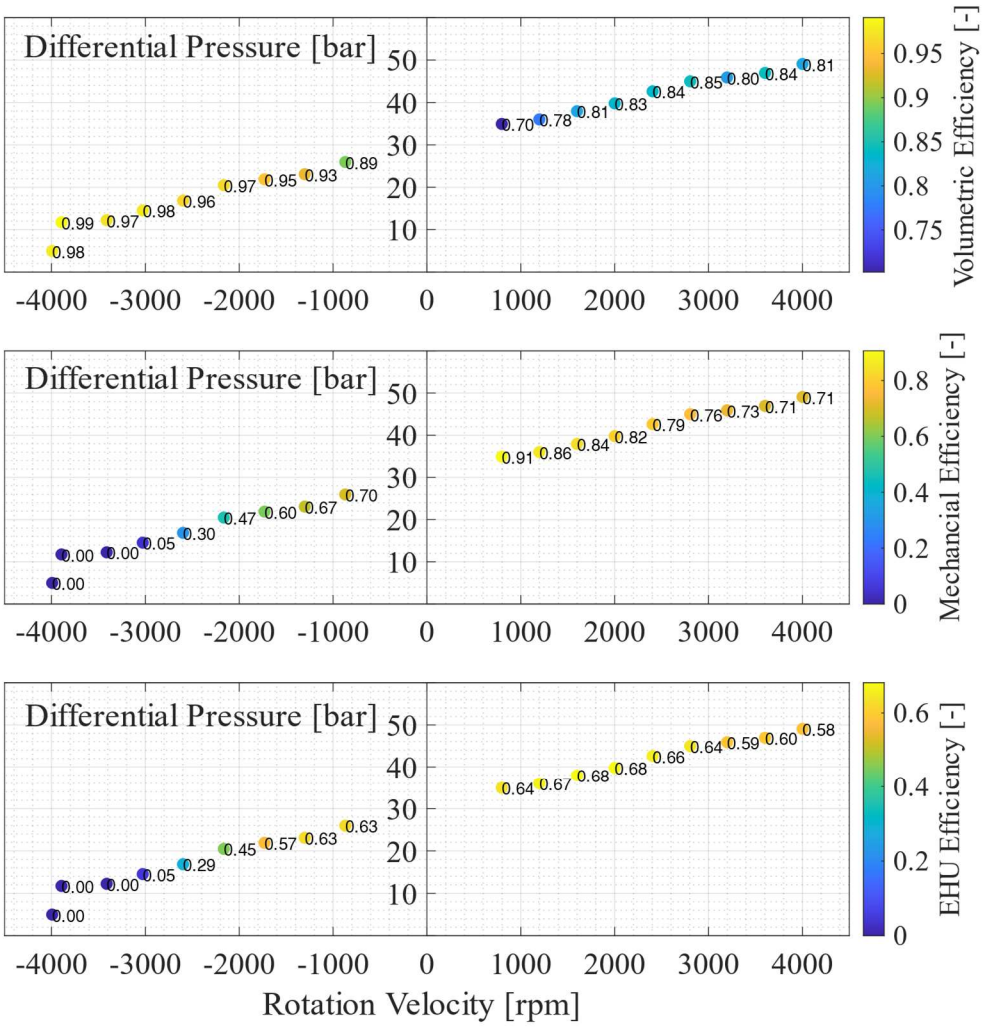

Figure 53: EHU efficiency performance in the demonstration

4.3 IGM model

In budget period 2 the model dedicated to internal gear machine has been completed. Conceptually, it may resemble the model dedicated to EGM, but the crescent, the difference between internal and external gear, and all the morphological differences constituted a challenge that had to be addressed. For the sake of clarity, the model conceptual schematic is reported in Figure 54.

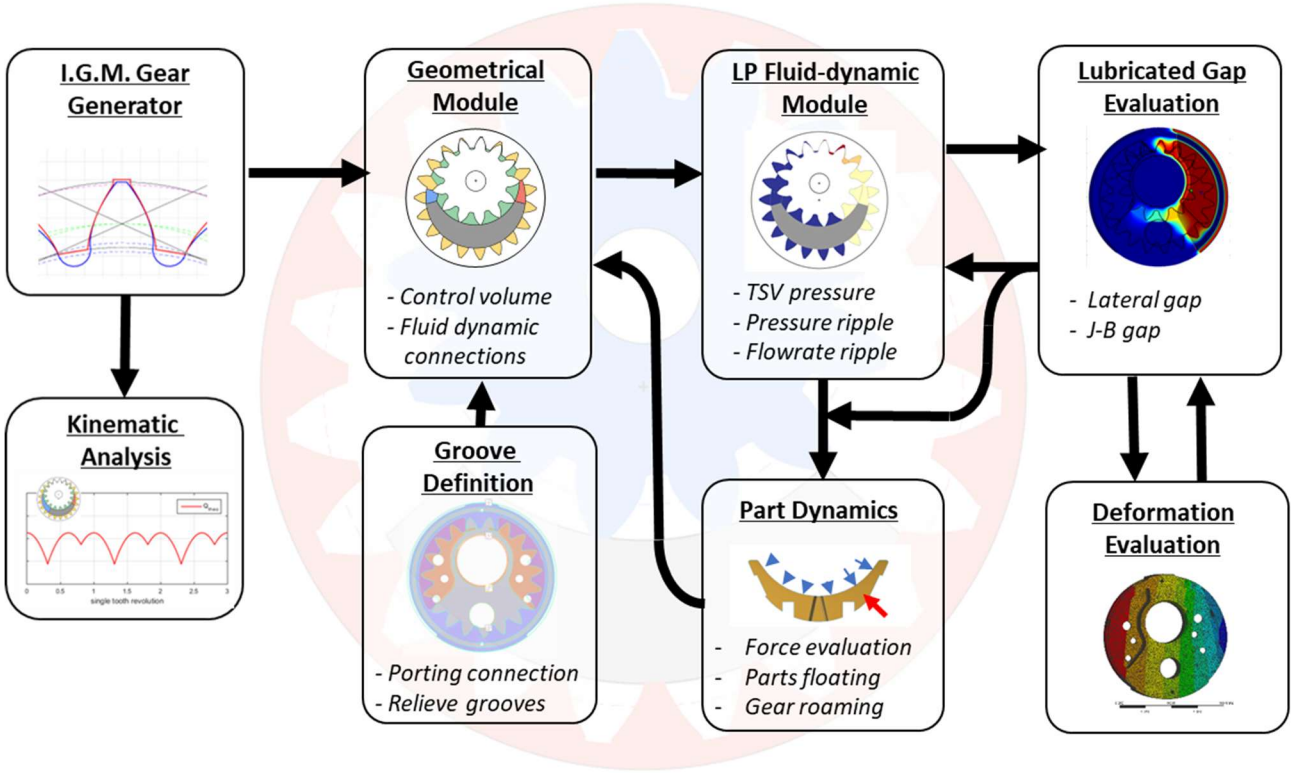

Figure 54: IGM model conceptual schematic

IGM Gear Generator. This submodule of the model takes as input some parameters defined by the user to generate the pinion and ring gear profile. Additionally has the capability of performing a kinematic analysis and calculate the kinematic flowrate output by the IGM.

Geometrical Module. The gears profile generated in the IGM Gear Generator is input into the geometrical module, where the internal volume of the HM is partitioned in many sub-volumes. In this module the volume of the sub volumes and the areas connecting them are calculated.

Groove Definition Module. This module is coupled with the Geometrical Module, and it calculates the connections of the internal volumes of the IGM with ports and grooves.

LP Fluid Dynamic Module. This module collects the data calculated by the Geometrical Module and the Groove Definition module to create the equivalent hydraulic circuit of the pump. When the equivalent hydraulic circuit of the pump is built, the pressure in all the internal sub-volumes and the flow exchanged between them is calculated.

Part Dynamics Module. Given the pressure distribution in all the internal volumes of the HM, the Part Dynamic Module calculates the forces and the consequent position of the parts.

Lubricated Gap Module. This module uses a CFD approach to solve the Reynolds equation and determine the pressure field, the gap height field, and the leakages generated the lateral gap.

Deformation Module. With this module the deformation of parts such as the gears and the lateral plate are evaluated. The deformation is then used to improve the accuracy of the calculation regarding the lubricated interfaces.

4.4 2nd generation EHU design

This paragraph describes the accomplishment of the milestone named "EH-unit design (2nd gen)".

The study performed through the Pugh chart in BP1, produced a very novel morphology for the 2nd generation EHU. The morphology offers advantage in compactness and component reduction, but also presents challenges that must be addressed carefully design every single part. To ease the understanding of how the parts work together and the understanding of possible issues that can emerge in the testing phase, it was decided to divide the design process in two and therefore produce two samples of the 2nd generation EHU. The two samples, named sample A and sample B, resemble one each other except two main differences. The first difference is that sample A does not have axial compensation system. The axial compensation system, even if apparently simple, is a HM feature that requires a very thorough design and can introduce a good amount of uncertainty in the results of a prototype. Since the axial compensation system role is to reduce the lateral gap, mitigate the leakages and improve the volumetric efficiency, the production of the sample A is proposed to prove the functionality of the concept more than the potential in terms of efficiency of the unit. The sample B, which features the axial compensation system, should show better efficiency. The second difference between the two samples lays in the rotor. Sample A feature a metal sleeve surrounding the rotor permanent magnets to protect them, while sample B has protrusion in between the magnets that alleviate the shear stress applied to the adhesive that weld them to the rotor lamination. In Figure 55 are shown the sample A and B HM and rotor.

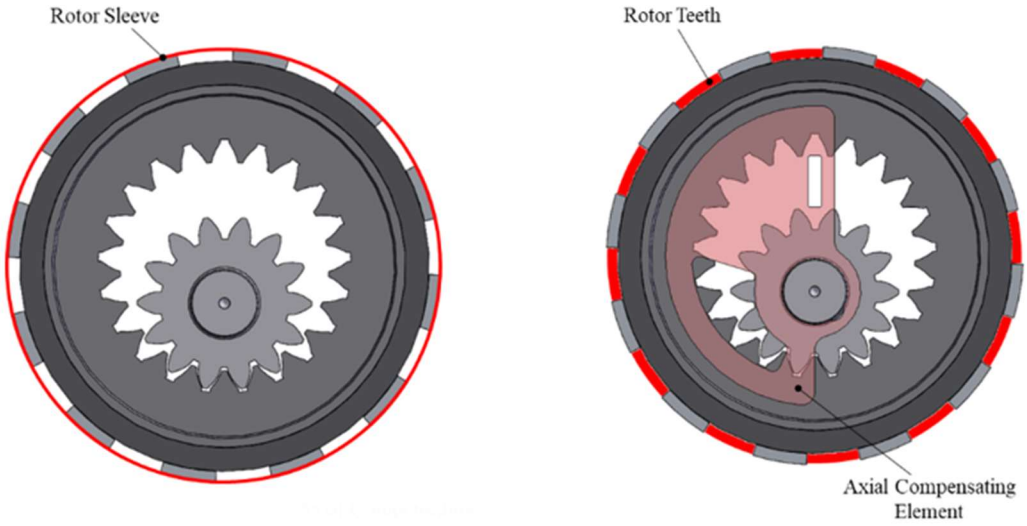

Figure 55: Left: sample A HM and rotor; right: sample B HM and rotor

Because of the supply chain issues generated by the world pandemic and the time constraints imposed by the project only the sample A was manufactured and tested.

4.4.1 IGM Power Loss Calculator

To design the IGM used in the 2nd generation an optimization procedure based on a genetic algorithm is set up. In this case, to evaluate a higher number of designs a simplified model dedicated to the HM was generated and coupled with the EM model. The HM model accounts for volumetric and mechanical losses.

To calculate the volumetric losses, three main sources of leakages are identified: the lateral leakage, which is the leakage between one TSV and the adjacent through the lateral gap; the tooth-tip leakage, which is the leakage between the gears tooth-tip and the crescent surface; and the drain leakage, which is the leakage happening between a TSV and the journal bearing. There, the leakages are calculated with the Poiseuille-Couette equation, assuming the gap constituted by two parallel plates, and the leakage flow laminar.

The hydromechanical losses are calculated as the result of several components. First, the shear torque generated in the journal bearing is calculated using the Petroff's equation. Then, a numerical integration procedure is used to calculate the shear torque generated on the lateral surface of the gears.

4.4.2 IGM gears profile optimization

The simplified model used to calculate the losses is then used to calculate the quality of the designs generated by the optimization with respect to some objective functions. In this case the objective functions aim to maximize the efficiency in pumping mode at maximum rotation velocity and maximum differential pressure and to maximize the power density of the design.

In addition to the objective function, also some constraints are imposed to guarantee the robustness of the gear set and ensure the complete filling of the HM also at high rotation velocity.

More precisely, to guarantee the robustness of the gearset the safety factor of the pinion teeth at bending and pitting together with the pinion shaft safety factor are calculated. To guarantee the filling of the HM the mean inlet velocity is constrained below a certain value. With these settings the optimization is performed and a pareto front shown in Figure 56 was found.

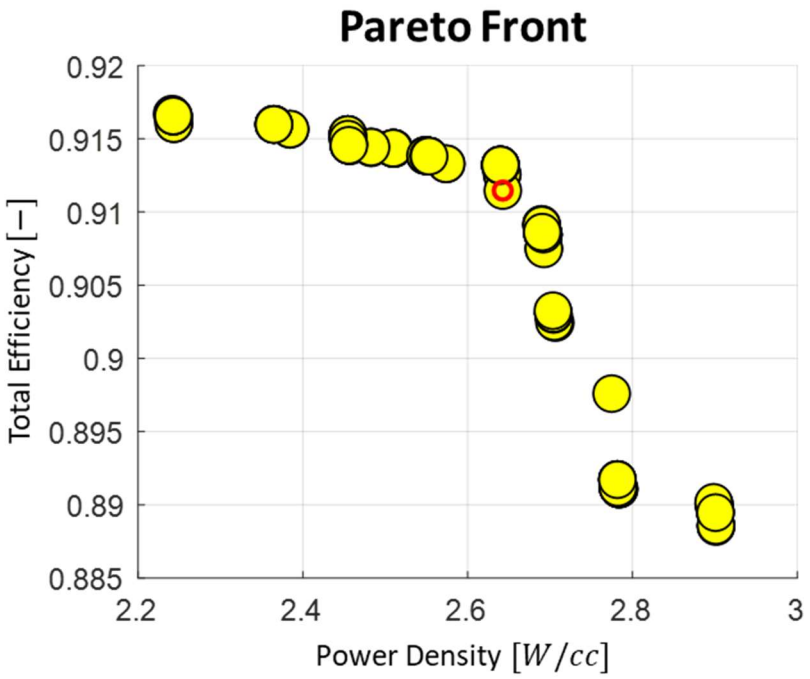

Figure 56: Pareto front obtained by the optimization process dedicated to the 2nd generation EHU

From the pareto front reported in Figure 56 a EHU design is selected. For completeness the parameters identifying the design are reported in Tab. 7.

HM Parameter		EM Parameters	
Pinion no. of teeth [-]	14	Rotor lamination material	M15
Ring gear no. of teeth [-]	21	Stator lamination material	M15
Gear axial length [mm]	12.72	Perm. magnets material	Sm2Co17-R30S
Pinion modulus [mm]	3.99	Conductor material	Copper
Ring gear modulus [mm]	4.11	Pole pairs [-]	6
Drive pressure angle [deg]	14.9	Depth of inert region [mm]	66.5
Pinion addendum radius [mm]	32.00	Depth of rotor back iron [mm]	7.90
Pinion dedendum radius [mm]	24.54	Magnets depth [mm]	4.54
Ring gear dedendum radius [mm]	42.25	Air gap [mm]	3.00
Ring gear addendum radius [mm]	38.23	Depth of tooth base [mm]	22.30
Pinion root fillet radius [mm]	1.40	Tooth fraction [-]	0.62
Pinion shaft radius [mm]	12.50	Depth of stator back iron [mm]	12.09
Gear interaxis [mm]	12.58	Permanent magnets fraction [-]	0.77
Pinion JB clearance [mm]	0.04	Active length [mm]	93.46
Ring gear JB clearance [mm]	0.08	Peak found. cond. dens. [cond/rad]	47.70
		Coeff. of 3rd harmonic cond. dens.	0.34

Table 7: Parameters of the 2nd generation EHU

4.4.3 IGM morphology and cooling system

To design the unit many fluid-dynamic and mechanical details were take in consideration, however, for the sake of brevity below is described the morphology of the unit and the EM cooling system only, since it represents the main novelty of the design.

In Figure 57 is presented the cross section of the EHU, where it is possible to see all its component. The unit has a cylindrical shape, and it is enclosed by two end-lids at the extremes. On the front end-lid is possible to find the ports of the EHU, on the opposite end-lid is placed the encoder that monitors the position of the rotating parts. On the inside of the end-lids are attached the front and bottom HM casing. On the bottom HM casing is press fit the liner that constitutes with the drive flange the JB system that supports the ring gear and the EM rotor. More precisely, the ring gear is press fit in the inside of the drive flange and positioned between the two HM casing, the rotor instead is press fit on the outside of the drive flange. In correspondence of the rotor of the EM rotor, the EM stator is press fit inside the external casing of the unit. In the image is also possible to see the pinion inside the ring gear and the low- and high- pressure volumes.

The EM cooling system is based on an additional passage that connects the high-pressure volume to the low-pressure volume through the EM casing. More precisely, two calibrated orifices connect the HP volume to the electric machine casing. These orifices allow a small part of the high-pressure fluid to go in the casing of the electric machine. To ensure the continuous intake of fresh fluid it is machined an opening that connects the EM casing to the low-pressure volume of the EHU. The calibrated orifices and auxiliary openings are highlighted in Figure 58.

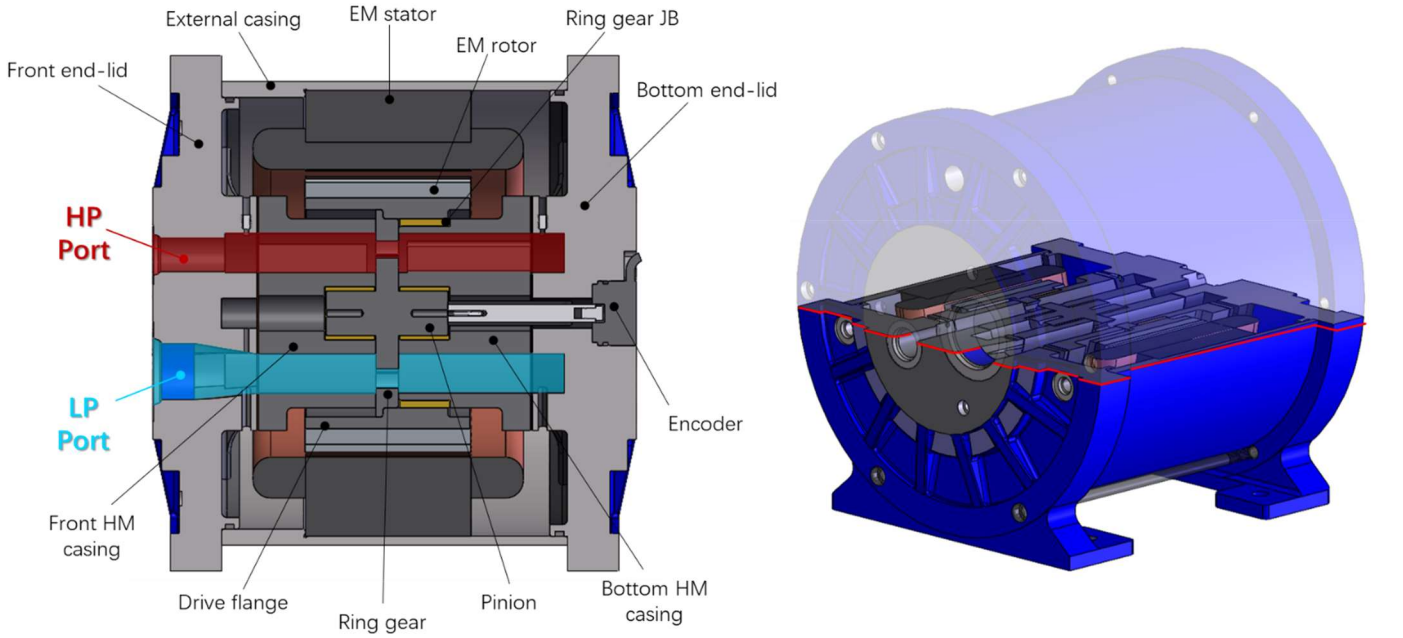

Figure 57: 2nd generation EHU sample A cross section with components label

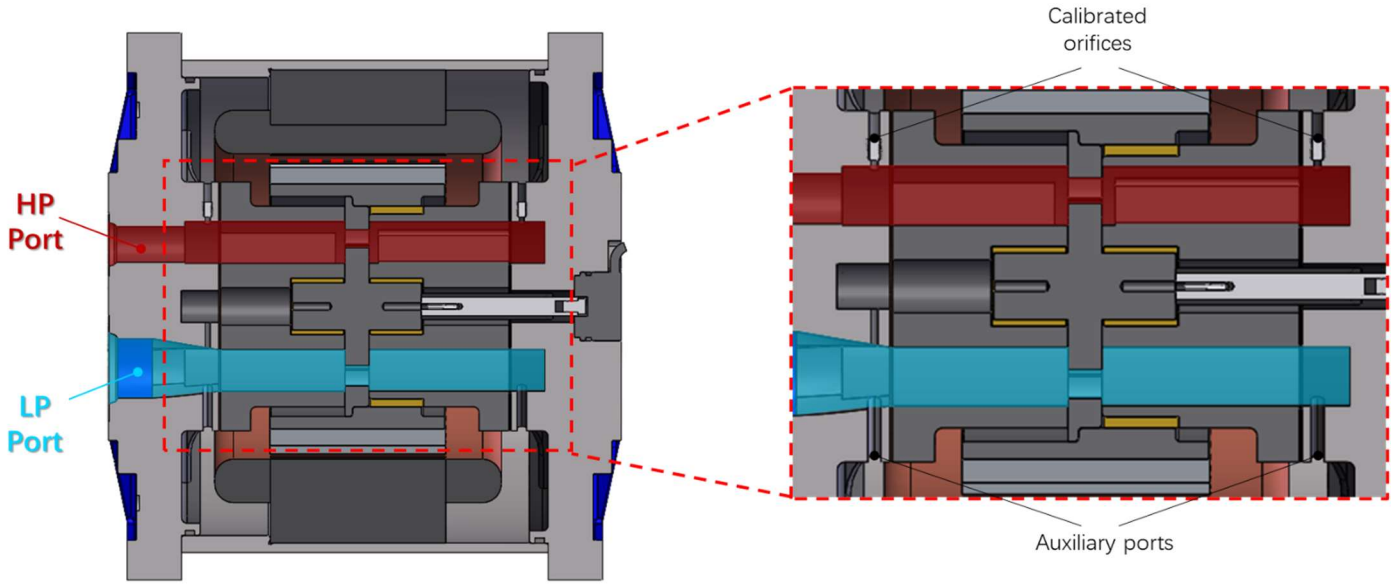

Figure 58: Cross section of 2nd generation EHU highlighting the internal openings that constitute the EM cooling system

To ensure the proper recirculation of the fluid several simulations were performed with a CFD approach. In Figure 59 is shown the control volume that contains the working fluid in the EM casing. The results of the simulations highlight the fact that there is a perfect recirculation of the fluid in the EM casing, and no hot spot can be identified.

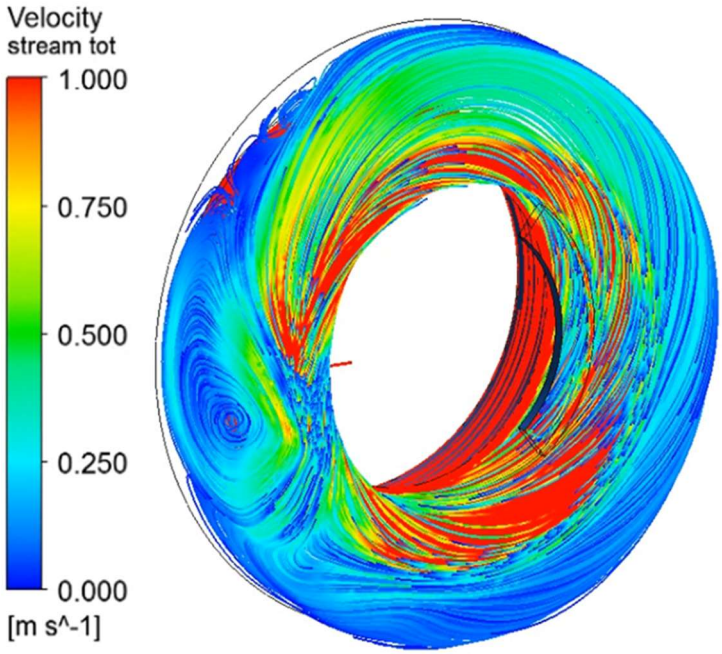

Figure 59: Fluid control volume and simulated velocity streamlines of the working fluid

4.4.4 IGM manufacturing and testing

After the design phase the EHU was manufactured and tested. In Figure 60 are reported the pictures of some of the parts of the 2nd generation EHU.

After machining the parts the EHU was tested with the same hydraulic circuit reported in Figure 37 and Table 5. During the experimental test the following volumetric efficiency was measured.

Looking at the volumetric efficiency is possible to notice that the trend is a suspected. Increasing the rotation velocity while keeping the pressure constant the volumetric efficiency increases. This is because the flow resistance generated in the lubricated gap increases, mitigating the leakages and decreasing the volumetric losses. If the rotation velocity is kept constant and the differential pressure increased instead the volumetric efficiency decrease. This is due to the increased action of the differential pressure on the leakages.

Figure 60: Top row, from left to right: EHU end-lid; EM rotor, pinion and radial compensation system; EM rotor with highlight of the metal sleeve protecting the magnets. Bottom row, from left to right: bottom HM casing with axial compensation system; EM stator; bottom end-lid.

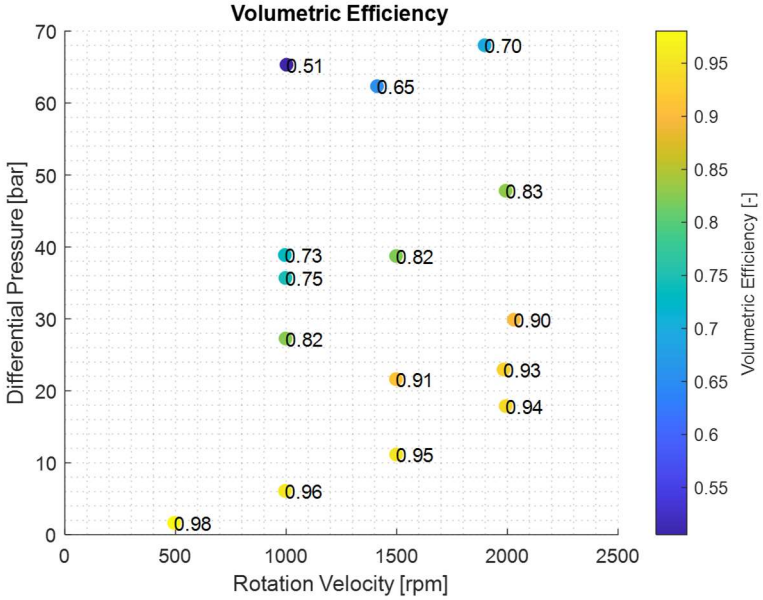

Figure 61: 2nd generation EHU volumetric efficiency

In general, is possible to see that the values of volumetric efficiency are lower than a commercial unit. This should not surprise since the EHU do not feature any axial compensation system and the many parts involved in the assembly do not allow a tight control of the lateral gap

height. The stack up tolerance analysis performed at room temperature and assuming an operating temperature of 70°C is reported in Figure 62.

	Dimension	Bilateral Tolerance	Temp.
A	-12.72	0.01	-12.728
B	-66.22	0.01	-66.295
C	-0.95	0.01	-0.951
D	-19.81	0.01	-19.816
E	195.3	0.025	195.300
F	-19.81	0.01	-19.816
G	-0.95	0.005	-0.951
H	-74.63	0.01	-74.715
Total Gap	0.21	0.035	0.028
Min Gap	0.175		-0.008
Max Gap	0.245		0.063

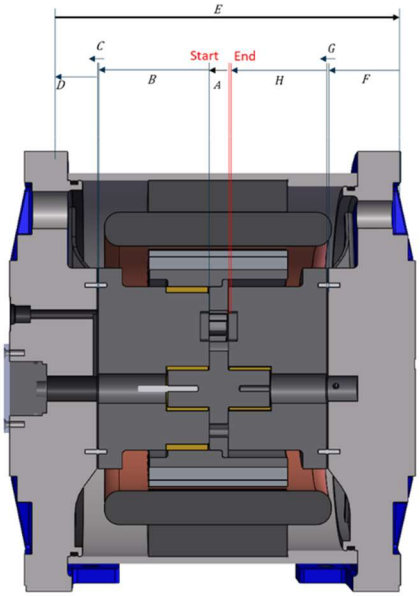

Figure 62: 2nd generation EHU parts dimension at room temperature, applied bilateral tolerance and dimension at operating temperature of 70°C

From Figure 62 is possible to see that at room temperature and considering the tolerances imposed on the parts, the total lateral gap can be between 175 and 245 microns (first column in Figure 62). However, when the temperature of the unit is brought to 70°C the parts expand and reduce the gap to a maximum height of 63 microns (second column of Figure 63).

With these results, not only the functionality of the EHU is proved, but also the accuracy of the model can be tested. To test its accuracy the 2nd generation IGM is simulated imposing different values of lateral gaps. With a lateral gap of 156 microns is possible to match the volumetric efficiency with an average error of 2%.

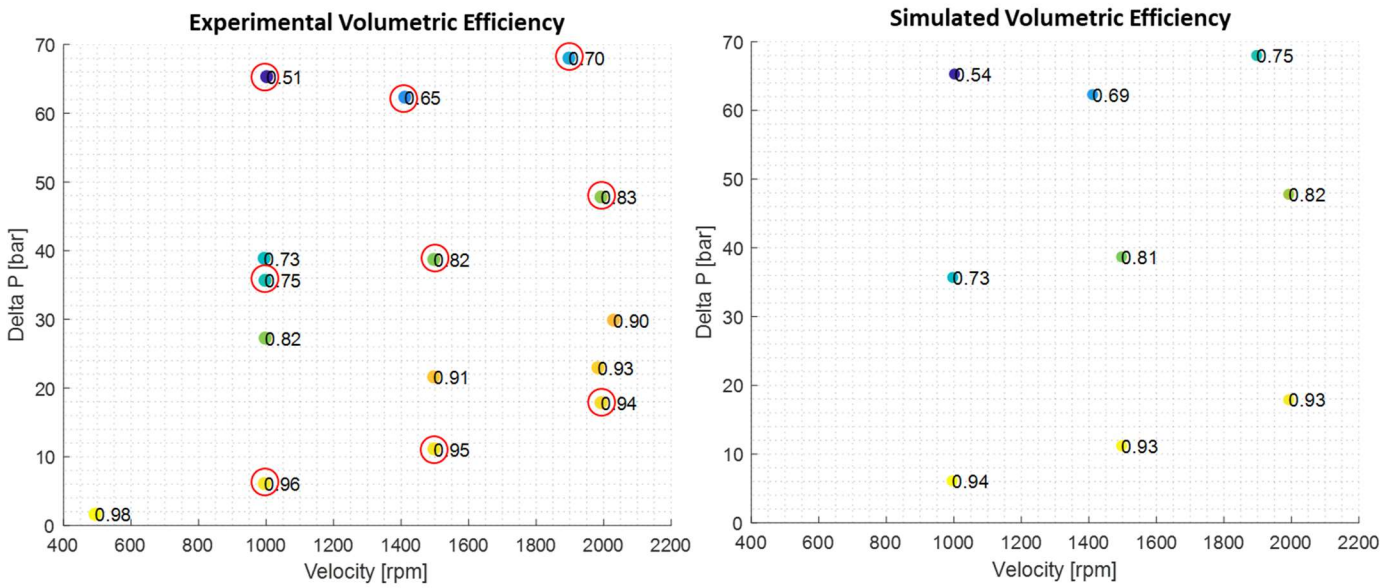

Figure 63: Comparison between experimental and simulated volumetric efficiency

Imposing a lateral gap of 156 microns implies the assumption of a temperature value for the parts that is in between ambient temperature and 70°C, which is a very reasonable assumption. With this comparison also the IGM model developed in the project is validated.

4.5 EHU design conclusion

This paragraph describes the accomplishment of the milestone named "EH-unit general design rules".

The design of two different generation of EHU allowed the gain of remarkable knowledge and the definition of guidelines that can be used from any designer engaged in the design of electro-hydraulic unit.

First, EHU are composed by an HM and EM. The definition of the optimal rotation velocity is a crucial aspect of the design, and it is the result of a tradeoff between HM and EM performance. While the EM would tend to rotate at higher velocity to increase the compactness and reduce the resistive losses, the HM may suffer for incomplete filling or excessive hydromechanical losses generated in the lubricated gaps. Both the optimization processes used in the process processes established an ideal rotation velocity for EHU in the range of 50-100 L/min between 4000 and 4500 rpm.

Additionally, the design effort put in the EM design highlighted that the machines characterized by a greater radius can develop more torque with the same amount of conductor, making designs with a large axial length-diameter ratio preferable.

The optimization performed on the 1st generation EHU pointed out some relations between geometrical parameters of the EHU and its performance:

- Larger EM, lower current density, higher efficiency
- Larger dedendum radius produce more shear losses

- More teeth reduce the flow ripple
- Positive correction factor increases torque ripple
- More shear losses require larger electric machine

The presence of the EM set some constraints on the material of the parts. To avoid the exacerbation of undesired leakages of electromagnetic flux cast iron must be avoided in proximity of the EM windings. To avoid the shortcutting of the EM laminations, and to withstand the generated torque value steel is recommended for EM stator casing and EM rotor drive flange.

It is of paramount importance the identification of the crucial dimensions of the parts the application of tight tolerances.

Finally, it is recommended that the seals used in the axial compensation system are prototyped with the state-of-the-art technology, which is represented by NBR or buna-N 3D printing machines.